I hereby give permission for public access to my thesis and for any copying to be done at the discretion of the archives librarian and/or college librarian.

_____

Alicia Ayars   May 2005

Detecting Hemlock Woolly Adelgid (*Adeleges tsugae*) Impacts on

Eastern Hemlock (*Tsuga canadensis*) Stands in the Quabbin Reservoir

Watershed Using AIMS-1 Imagery

by:

Alicia Tomlinson Ayars

A paper presented to the

Faculty of Mount Holyoke College in

Partial Fulfillment of the Requirements

for the degree of Bachelors of Arts with

Honor

Department of Earth and Environment

South Hadley, MA 01075

May, 2005

This paper was prepared
under the direction of
Professor Thomas L. Millette
for eight credits.

ACKNOWLEDGEMENTS

TABLE OF CONTENTS

LIST OF FIGURES

LIST OF TABLES

ABSTRACT

The infestation of indigenous forest species by foreign pests plays an important role in ecosystem change, often altering stable stand composition and vigor. A recent and pressing infestation in the United States by a foreign insect is the hemlock woolly adelgid (*Adeleges tsugae*: HWA), attacking eastern (*Tsuga canadensis*) and Carolina hemlocks (*Tsuga caroliniana*). The eastern hemlock is a shade tolerant, late succession conifer and key component of Northeastern mixed forest stands. The adelgid kills eastern hemlocks by feeding on the xylem ray parenchyma cells and disabling the tree from producing allelochemicals which chemically defend plant tissue walls. Feeding changes chlorophyll production, with needles eventually turning gray and dropping. It was this change in chlorophyll vigor that this study sought to detect and characterize. As hemlocks die due to adelgid infestation, gaps in the canopy aid the growth and density of already abundant hardwoods, altering stand dynamics. Additionally, nitrogen held in the root systems of hemlocks is released into soils as death occurs. Nitrate leaching is a problem within the Quabbin Watershed because it is a public water supply watershed, and higher nitrogen rates degrade the quality of water.

Hemlocks and adelgid infestation were analyzed in images captured by the Airborne Imaging Multispectral Sensor (AIMS-1) in April of 2004 during leaf senescence of hardwoods. AIMS-1 collects data within the visible spectrum and near infrared spectrum of light using 3 multispectral bands: near infrared, red and green. Healthy vegetation reflects light in the near-infrared (NIR) band between $0.62\mu m$ and $0.7\mu m$ and absorbs red energy between $0.45\mu m$ and $0.66\mu m$. As parenchyma cells accumulate, the chlorophyll content of plants increases, causing plants to absorb more light energy in the red band and reflect more energy in the near infrared band. The reduction of parenchyma cells should provide a direct link between infestation and corresponding changes in the absorption and reflectance properties of damaged hemlocks. The plots used in this study had previously been classified by the Division of Water Supply Protection, which is part of the Massachusetts Department of Conservation and Recreation, as possessing adelgid damage, so tests focused on classifying hemlock vigor tree by tree. This was done in order to first assess if AIMS-1 data preserved spectral differentiation within two broad classes of health: damaged and healthy. Tests show a statistically significant difference in spectral response between the two classes in the 8-bit data. The vegetation class with the tightest spectral fit is the Transform Normalized Difference Vegetation Index (TNDVI). Percentages of stands can be delineated manually due to the high spatial resolution of the image; however supervised classification does not provide any information about individual tree health. 10-bit data used in this study does not lend any more useful information about the spectral differences of damaged hemlocks. Future work will attempt to characterize entire stands of damage rather than individual trees so foresters may be able to implement treatment options typically conducted at the stand level.

INTRODUCTION

The infestation of indigenous species by foreign insects plays an important role in forest change. As pests are introduced into an ecosystem, they alter current and stable stand composition and vigor. Pathogens spread to new areas, degrade their host species, and increase ecosystem susceptibility to further disturbances (Orwig, 2002). Degradation due to the introduction of pests can continue unabated in the absence of information regarding its spread and impact.

A pressing infestation in the Eastern United States by a foreign insect is the hemlock woolly adelgid HWA (*Adeleges tsugae*), attacking the eastern hemlock (*Tsuga canadensis*) and Carolina hemlock (*Tsuga caroliniana*). While proving deadly for the eastern and Carolina hemlocks, the woolly adelgid does not affect western hemlock (*Tsuga heterophylla*) or Chinese hemlock (*Tsuga chinesis*). The eastern hemlock is a key component of mixed forest stands in the Northeastern United States. It ranges throughout New England, New York, Pennsylvania, the Mid-Atlantic states, and in smaller quantities farther to the south. It can also be found in Nova Scotia across southern Ontario, northern Michigan and northeastern Minnesota.

The hemlock is a shade tolerant, late succession conifer, strongly represented in climax forests because of its lifespan of up to 400 years (Bonneau et al, 1999a). Because of the hemlock's longevity and propensity for shade, it can

live in suppressed environments with low levels of sunlight or heavily moistened soil, and change surrounding microclimates in order to prolong its life (Goerlich & Nyland, 1999). The dense canopy of the hemlock intercepts all manner of natural elements, including but not limited to solar radiation, precipitation, and wind (Evans, 1995). In this manner hemlock stands perpetuate their distinctive environments and provide rich habitats for at least eight bird and ten mammal species (Yamasaki et al, 1999).

In the past, the eastern hemlock was an important member of Northeastern mixed forest stands. Approximately 5,000 years ago an unknown pathogen caused hemlock populations to decline unexpectedly throughout North America (Orwig & Foster, 1998). This decline caused ecosystem changes similar to those occurring throughout the eastern United States, as the population died and then returned. The hemlocks' return was large, and before European settlement hemlock stands covered much of the northeast (Foster and Aber, 2004). Estimates from 1814 to 1815 show that hemlocks comprised at least 19.9% of trees in United States forests. By 1973, that percentage had fallen to 5.8% of total trees in the United States. Old-growth hemlock was exploited for both its bark and wood. Today the hemlock population is still around 5% of trees within the United States (Quimby, 1995). It is an important member of the New England forest landscape, though, and is estimated to account for between 61% - 70% of all softwoods in Connecticut (Bonneau et al, 1999a).

Jenkins, Canham, and Barten (1999) report that as hemlocks die, gaps in the canopy allow greater light to penetrate the forest floor, aiding in the growth and density of already abundant hardwoods. Studies suggest that hemlocks are most readily replaced by black birch (*Betula lenta*) and red maple (*Acer rubrum*) (Bonneau et al, 1999a). Further adding to changes in forest stand composition, invasive species including Japanese barberry (*Berberis thunbergii*) and honeysuckle (*Lonicera japonica*) are quickly replacing defoliated hemlocks. Stands comprised of hemlock currently exist in three types: pure hemlock, hemlock mixed with dominating white pine, and hemlock mixed with dominating hardwoods (Division of Water Supply Protection (DWSP, 2004)). Hemlock infestation and death compromises these unique stand structures and have researchers predicting a complete change in cover type from hemlock to hardwood-dominated forests (Orwig & Foster, 1999).

Hemlocks are usually located on steep hillsides in riparian areas, shading trout streams for spawning and providing shelter for animals. Hemlocks have shallow root systems, which makes them highly susceptible to disturbances of any kind. Trees on mountain tops with poor, dry soils are most susceptible to infestation when compared to those in riparian zones (Orwig & Foster, 1998).

Approaches to managing the woolly adelgid always result in changes to the forest floor and surrounding ecosystems. Being located primarily in riparian zones, hemlocks provide shade for rivers and lakes. Accompanying hemlock mortality, stream temperatures rise due to sun exposure threatening habitat

quality. Nitrate leaching and cation losses pose serious problems for organisms living within and around hemlock stands as well because hemlocks sequester nitrogen by storing it in their root system. Once the hemlocks die this nitrogen is released back into the soil. Jenkins, Aber, and Canham (1999) noted that forests comprised of degraded hemlock stands experienced nitrification rates 30 times higher than hemlock stands without infestation. Kizlinski et al. (2002) report net nitrification rates 41 times higher in woolly adelgid damaged sites, 72 times higher in recent hemlock harvests, and over 200 times higher in old harvests when compared with undamaged hemlock sites which had near-zero nitrification rates. Mortality tends to increase soil moisture and subsurface flow because the hemlock is no longer providing shelter with foliated branches. This allows for the increasing movement of released nutrients to streams. The result is water pollution because of increased phosphorous and lower nitrogen levels in the soil, which affects productivity.

Hemlock Woolly Adelgid

The hemlock woolly adelgid is an exotic pest, originating in Japan that feeds on the needles of eastern hemlocks (Battles et al, 1999). *Adelges tsugae* was brought to the Pacific Northwest in 1924, next appearing in Virginia in 1951. It has since migrated north, reaching Connecticut in 1985. By 1995 the woolly adelgid had spread to 11 states from North Carolina up the eastern seaboard to Massachusetts. It has caused mortality in at least 5 states including Virginia,

Pennsylvania, New Jersey, New York, and Connecticut (McWilliams & Schmidt, 1999).

The woolly adelgid is parthenogenic, meaning that all adult females are capable of reproducing (DWSP, 2004). Females produce more females from unfertilized eggs, which is a very fast way of reproducing a population. Adults typically lay between 50-300 eggs, with an average of 100 eggs per bearing adult. Each adult female produces eggs twice a year, in the spring between March and April and again in mid-June. The second generation, hatched in June, is migratory and moves to spruce with no evidence of spruce being able to support the adelgid (Souto, 1995). The adelgid spends winter feeding in order to grow and breed again in the spring and summer.

(*Figure 1*): The woolly adelgid attached to hemlock needles. Notice the white woolly substance.

The woolly adelgid is a small (1-2mm) aphid-like insect, whose name originates from the white woolly substance it secrets during winter (Figure 1) (Royle & Lathrop, 1997). The adelgid settles at the base of the hemlock needle then inserts its stylet into the needle, feeding on the fluids in xylem ray parenchyma cells. Stylet insertion is generally intracellular near the adaxial side of the needle and proximal to the abscission layer (Young et. al, 1995). Once

inserted into the plant, the stylet generally moves between cells before penetrating the xylem ray parenchyma cells insides.

In addition to sucking out the trees' cells, the adelgid injects toxic saliva into the branch, further hastening the death of the hemlock (Royle & Lathrop, 1997). The saliva is used to guide the stylet through the cells and is then left behind because adelgid stylets do not have separate canals for feeding and salivary processes.

The stylet bundle includes four stylets: two outer mandibular stylets and two inner maxillary stylets. The mandibular stylets house the maxillary stylets which extend and retract, acting as the feeding mechanisms. The stylet lengths of nymphs have been measured at up to 5 times their body length, but as the adelgid grows in size, the stylet length generally does not increase (Shields et al, 1995). It is hypothesized by Young et al. (1995) that the stylet is adapted not only for feeding but for anchoring the adelgid to the feeding site.

The presence of adelgids at high densities prevents the production of new hemlock growth the following year (Souto et al, 1995). Within the first year of infestation, the adelgid depletes the hemlock of its youngest growth. The following year adelgids are forced to feed on the older growth, causing a reduction in their survival rates. This also causes a greater number of developing nymphs to die without first reproducing because there is no available host to feed on. Adelgids that die as nymphs before reproduction are called sexuparae. A pattern is established where populations climax during the first year of infestation

while hemlocks are still producing new needles. Adelgid populations then collapse the second year when hemlocks are too damaged to reproduce new growth. During the third year of infestation 11% to 15% (Souto et. al, 1995) of hemlock buds produce new growth, rebounding from the adelgids' slowed feeding rates the second year. Adelgids quickly monopolize the new growth and resurge to a second population peak only to decline again during the fourth year of infestation when most trees die (Yorks et al, 1999). Following the first year of colonization, more than 93% of adelgids produced sexuparae; in the fourth year only sexuparae are produced (Souto et al, 1995). That being said, hemlocks have lived with infestation for over a decade in weakened conditions (RCE, 2002).

The adelgid's preference for new growth can be attributed to lower nutrient contents in older plants (Miles, 1990). Additionally, with age a plant's allelochemical content within the tissue increases. Allelochemicals act as chemical defenses for plants' tissue walls, making feeding for the adelgid more difficult. Young hemlock trees have not developed the elevated levels of chemical protection that older generation trees have, so they fall more easily to the adelgid. There is also evidence that the saliva of the adelgid prevents the chemical defenses of the plant from replacing itself. The adelgid accomplishes this by absorbing the allelochemicals before the damaged cells.

There are no natural predators of the woolly adelgid in the United States. The winter mortality is high and has been noted at 75% by the Division of Water Supply Protection within Massachusetts, but the rapidity with which the adelgid

reproduces allow population growth to occur. Orwig et al. (2002) reported that mortality is weakly correlated to stand aspect and stand size. He concluded that, as the adelgid increases in numbers, external variables such as slope, elevation, and stand composition play increasingly smaller roles in controlling damage. The only environmental barrier that has been noticed is latitude (Orwig et al, 2002). Winter temperatures are lower in higher latitudes, and this cold factor prevents the adelgid from surviving. Winter mortality rates require temperatures below -30° C for extended periods of time (Orwig et al, 2002). If the adelgid manages to survive in such low temperatures their tolerance for the cold generally increases, allowing for future northern movement.

As a result of feeding, hemlock needles turn grayish in color and eventually drop. Infestation progresses from the bottom of the tree upwards and can be evenly distributed throughout the tree. The adelgid prefers younger foliage, so new growth is attacked as it is produced (DWSP, 2004). This new growth sprouts from the ends of hemlock branches, giving the appearance of a healthy vegetation ring around the trees. As infestation progresses hemlocks appear to be thinning until only a sparse amount of needles are left on the top of the trees crown.

Accompanying the infestation of hemlocks are changes in chlorophyll production. While thinning is noticeable throughout the process of death, measuring changes in chlorophyll vigor requires more than sight. Chlorophyll production and vigor appear within remotely sensed imagery utilizing

multispectral or colored bands. The chlorophyll content within plants increases with age because the internal parenchyma become denser (Guyot et al, 1989). Aged hemlocks should reflect the build up of parenchyma, but it is these cells that the adelgid feeds upon. Lower chlorophyll levels of trees infested by the woolly adelgid should relay different spectral responses in multispectral, broad band imagery than healthy, aged hemlocks that are building up xylem ray parenchyma cells. Noting woolly adelgid infestation is fundamental to preserving the health of hemlocks stands, and, through the utilization of remotely sensed imagery managers may note chlorophyll changes and recognize new invasions (Royle & Lathrop, 2002b).

Research Questions

There is a recognized need to research the woolly adelgid, as it is attacking and compromising forest stand structure and health. Quantifying damage through remotely sensed imagery is a cost-effective way of studying populations of trees without having to do time-consuming ground-truth work. In addition, the results yielded from remotely sensed images may provide more information than results attained by ground-truth methods because analyzing spectral response patterns within stands of healthy and damaged hemlock may reveal differing levels of chlorophyll (Royle & Lathrop, 2002a).

From a forestry standpoint, the identification of hemlock damage on a tree by tree basis is imperative in order to quantify the amount of damage within a

stand. Within the Division of Water Source Protection, once 50% of any area possessing hemlocks is infested, salvaging operations begin. Classifying damage through image classification was attempted within a small hemlock stand in order to test the spectral homogeneity of the damage classifications.

It was unknown at the inception of this study if the AIMS-1 sensor would preserve spectral and spatial differentiation to a great enough degree that health/ vigor differences between infested and healthy hemlocks and different degrees of infestation of hemlocks could be quantized. The study was completed using predominantly 8-bit imagery, and there were doubts as to whether the sensor in 8-bits provided enough quantized levels to discriminate between different damage classifications. This prompted the integral question of the study: *will infested hemlocks have statistically different maximum and mean spectral signatures when compared with healthy hemlocks*? Images have been taken in 10-bit format for areas of the Quabbin watershed and there was speculation that if spectral differences were not preserved in the 8-bit data, then perhaps the 10-bit images might lend more information. This question was not as important within the study as the 8-bit data proved to be useful. The question this prompted is the fourth in the study: *if 8-bit data cannot provide information and or quantify woolly adelgid damage, can 10-bit data provide any additional information*? The spatial characteristics of the sensor were important in this process because high detail imagery was necessary in order to identify hemlocks.

Research focused on separating and developing health classifications for eastern hemlocks infested by the hemlock woolly adelgid. Detecting these spectral differences is important because they convey useful information about the radiometric resolution of the sensor. Vegetation classes with relatively homogenous signatures can also lead to automated processes such as image segmentation which has the ability to generate tree health information on a much larger scale. To test the homogeneity of the spectral responses, a supervised classification was tested. This was important in the overall study and prompted question 3: *can adelgid infestation be quantified by percentage of stand damage?*

Another method of testing chlorophyll vigor within images is through the use of vegetation indices. In addition to testing chlorophyll vigor, vegetation indices remove background noise from the imagery such as soil moisture reflectance or aspect interference. Vegetation indices were used in this study to understand which damage class is the most homogenous, and which index removed the most background interference. This was tested in question 2 by asking: *which vegetation index will relay the most information concerning hemlock decline?*

Remote Sensing

A remotely sensed image is a two-dimensional array of numbers, each representing the brightness of a small elemental area in the digital image (Schowengert, 1983). When an object is struck by sunlight, that object can reflect,

absorb, or transmit the energy. What happens to the light after striking depends on the object's characteristics (Jensen, 2000). Materials that are dark absorb most light energy, and light materials reflect most wavelengths that have struck the object. By assigning numerical values to each quantized level of color, computers can process the reflectance and absorption properties of objects numerically.

Within remotely sensed images, thousands of light sensitive photosites (pixels) act as the converters of the wavelengths of light into electrical signals, which then assign the numerical reflectance value. Pixels are fundamental within digital images because the size of the pixel affects the detail within the image. As the pixel area is reduced, more scene detail becomes available. The amount of detail represented by the pixel is contingent upon the altitude of the sensor and its instantaneous field of view (IFOV). Bits represent the radiance for each pixel with only 5 to 6 bits required for a visually continuous image scene. Five-bit data is recognized as a minimum for continuous imagery (Schowengert, 1983) and represented numerically as 2^5 meaning that 2 x 2 x 2 x 2 x 2 represents the number of gray levels (32) in the data. Most commonly used is 8-bit data with 256 gray levels.

Gray levels are excellent indicators of change, but color imagery has become fundamental when analyzing vegetation. Multispectral images are taken simultaneously on alternate bands within the electromagnetic spectrum. Each pixel within a multispectral image carries x and y coordinates for location, but instead of a gray level, it recognizes the spectral coordinate or wavelength giving

it color. Figure 2 represents the visible, infrared, and middle infrared light

spectrums for which information is transferred onto multispectral bands. Images

can be taken utilizing any band combination; it is solely dependent upon the

capabilities of the sensor.
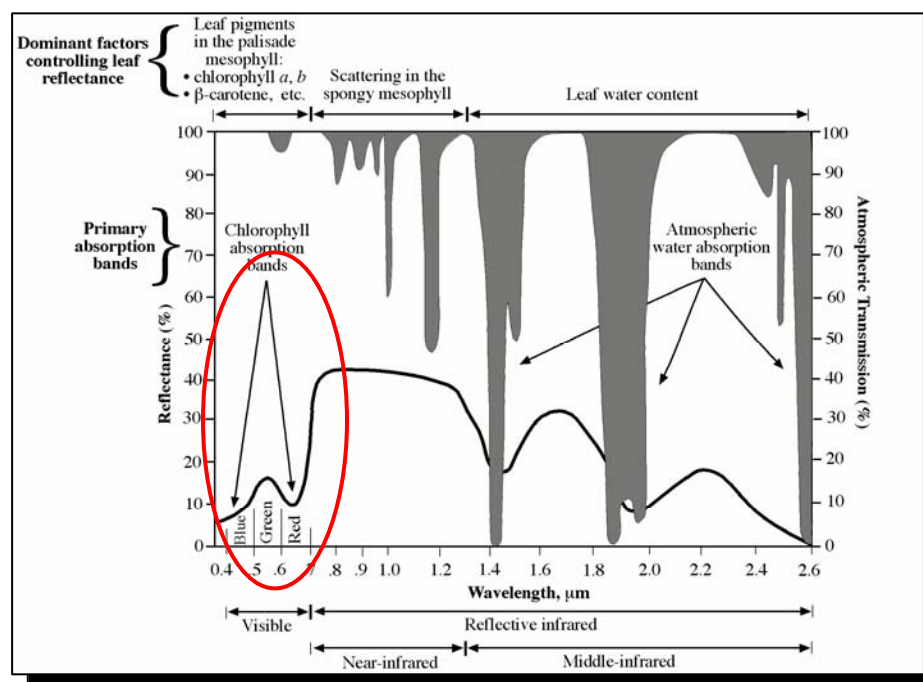
(*Figure 2*): The visible, near infrared, and middle infrared spectrums of light. The chlorophyll absorption bands are circled. Notice the sharp jump in reflectance as you near the infrared spectrum of light. In this study, the near infrared and red bands were focused upon.

All color systems for display of digital images utilize an additive color

composite system with three primary colors: red, green, and blue (RGB)

(Schowengert, 1983). When displayed as an RGB combination, images appear as

a standard color infrared (CIR) image. Color infrared is used as a good indicator

of plant vigor, and images in this study were taken using the AIMS-1 sensor

capturing data in visible green 0.54-0.59, visible red 0.64-0.69, and the near
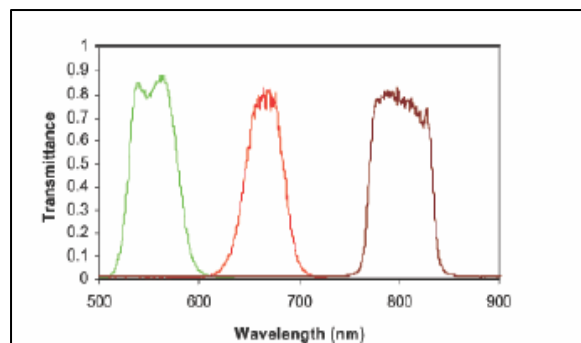
(*Figure 3*): CIR peaks of healthy vegetation along the visible spectrum of light, nearing the infrared spectrum.

infrared 0.78-0.84 micrometers respectively, matching Landsat TM data. Healthy vegetation reflects energy in the near-infrared (NIR) band, and absorbs energy in the red band. Chlorophyll is the most important plant pigment absorbing red and blue light.

Chlorophyll absorbs energy between wavelengths of 0.43 and 0.66μm (Jensen, 2000). This differs in the near-infrared region, as vegetation is generally characterized by high reflectance levels ranging from 40-60% of light, with 5-10% absorption, and the remaining light being transmitted to other leaves (Horler et al, 1983). These representations can be seen by the peaks in Figure 3. This figure is representative of the vegetation peaks within the sensor used for this study.

When a plant is under stress, chlorophyll production decreases causing a lack of green pigmentation, which typically causes the plant to absorb less energy in the absorption band. This causes a change in spectral response patterns. Stress induced changes in reflectance have been directly linked to chlorophyll content in numerous studies (Pontius, 2005).

A tree's optical properties are not defined solely by the leaves absorption and reflectance patterns, but can also be defined by a tree's bark and, in the case

of conifers, its cones. Within the visible spectrum of light, bark has a higher reflectance level than leaves; however, in the near infrared band the bark's reflectance is lower than leaf reflectance. When the leaf density decreases on the branch, either due to disease or senescence, the reflectance properties of bark become more important for analyzing the spectral response patterns. Also important is the effect of the underlying vegetation. In an open stand or during senescence, the soil beneath the trees can alter the responses recorded.

Spectral responses will range throughout an image, but trends emerge with respect to the landscape. In a forest, healthy plants will have roughly the same pixel reflectance value, and deep bodies of water are uniform and generally absorb all the light. When brightness values for pixels with similar values are combined, the mean value forms a group and a unique pattern. With these patterns in mind, the next step is to cluster features into similar classes and measure their spectral responses.

Assessing Hemlock Damage

In this study I question if infested hemlocks have different reflective characteristics when compared with healthy hemlocks, specifically in relation to changes in chlorophyll production, and if these differences are preserved in AIMS-1 data.

The answers to these questions will hopefully lead to the identification of infested areas through a variety of image processing techniques including image

segmentation and image classification. The function of image segmentation is to define regions within an image which correspond directly to the ground (Abeyta & Franklin, 1998). Image segmentation groups pixels based on the spatial domain of the image and the mutually exclusive groups of the image segmentation (Haralick, 1985). Segmentation is a quicker method of defining regions in an image, whether the pixel values are an exact fit or within a certain value range (Woodcock & Harward, 1992). While not as accurate as human interpretation, defining boundaries through segmentation will generate data about the entire Quabbin region rather than several small sample plots. The laboratory procedures used to test the sensor's ability to detect damage, while appropriate for the size of this study region, would be too time-consuming when applied to a larger forested area. Image segmentation would expedite the process of identifying damaged adelgid on an object by object basis. This technique could also be used over a period of time to evaluate the amount of forest structure change.

Classification is similar to image segmentation, as it is a process of sorting pixels into individual classes or categories of data. There are two types of classification procedures: supervised and unsupervised. An unsupervised classification generates the outcome image that displays all of the spectral signatures detected within the input image. In a supervised classification, the process uses reflectance values of predefined training sites chosen to represent the general characteristics of the variable being tested. If a pixel satisfies a certain set of criteria, then the pixel is assigned to the class that corresponds to that criterion

(Erdas Help, 2005). A supervised classification allows signature inputs to be the only parameters within the test, thereby limiting the outcome image to display the desired characteristics. There are drawbacks to working at the pixel level if the ground features are larger than the grain size, because the ability to identify objects decreases with each differing pixel reflectance (Winne, 1999). Image segmentation, while similar, is actually object based. This study is more focused upon tree by tree identification; however, image classification may provide useful information about the homogeneity and heterogeneity of the damage classifications spectral characteristics.

The answers to these questions will help to further explain the radiometry of the AIMS-1 sensor, which is a fundamental goal in this study. In the event that it proves possible to identify hemlock woolly adelgid damage through broadband multispectral imagery, such imagery can aid foresters in their management of the Quabbin watershed.

METHODS

Site Description

The study is located in the Quabbin watershed, North East of the Mount Holyoke College campus in Hampshire County Massachusetts, Lat $42^o21^'03^"$E, Long $072^o24^'11^"$N (Figure 4). The Quabbin reservoir serves as the drinking water supply for the greater Boston area, and the land in the watershed is intensively managed. Woolly adelgid infestation and its spread have been recorded by foresters working within the Quabbin. The forest is a Northeastern coniferous/ deciduous mix with the prominent tree types being white pine (*Pinus strobus*), red maple (*Acer rubrum*), black birch (*Betula lenta*), and white oak (*Quercus alba*).
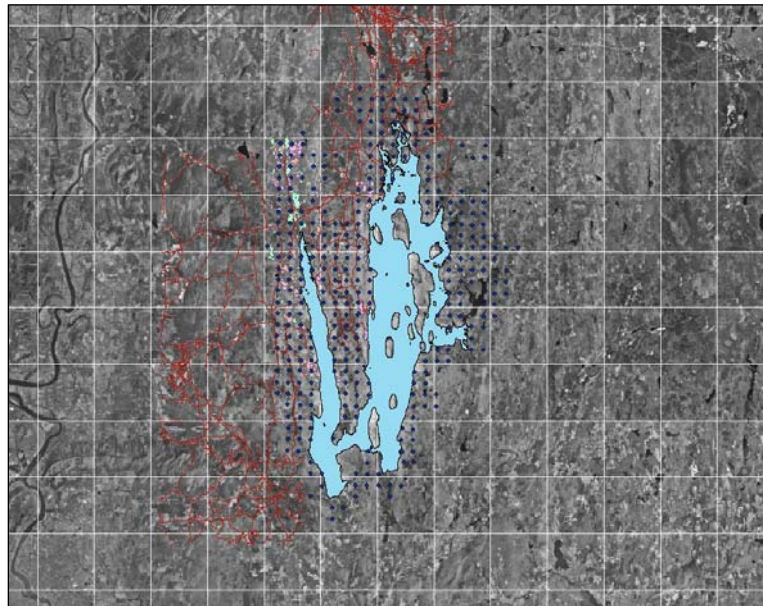
(*Figure 4*): GIS Image of the Quabbin Watershed. The blue dots represent Continuous Forestry Index Plots. Vegetation type polygons are on this map, but they are not visible.

The AIMS-1 Sensor
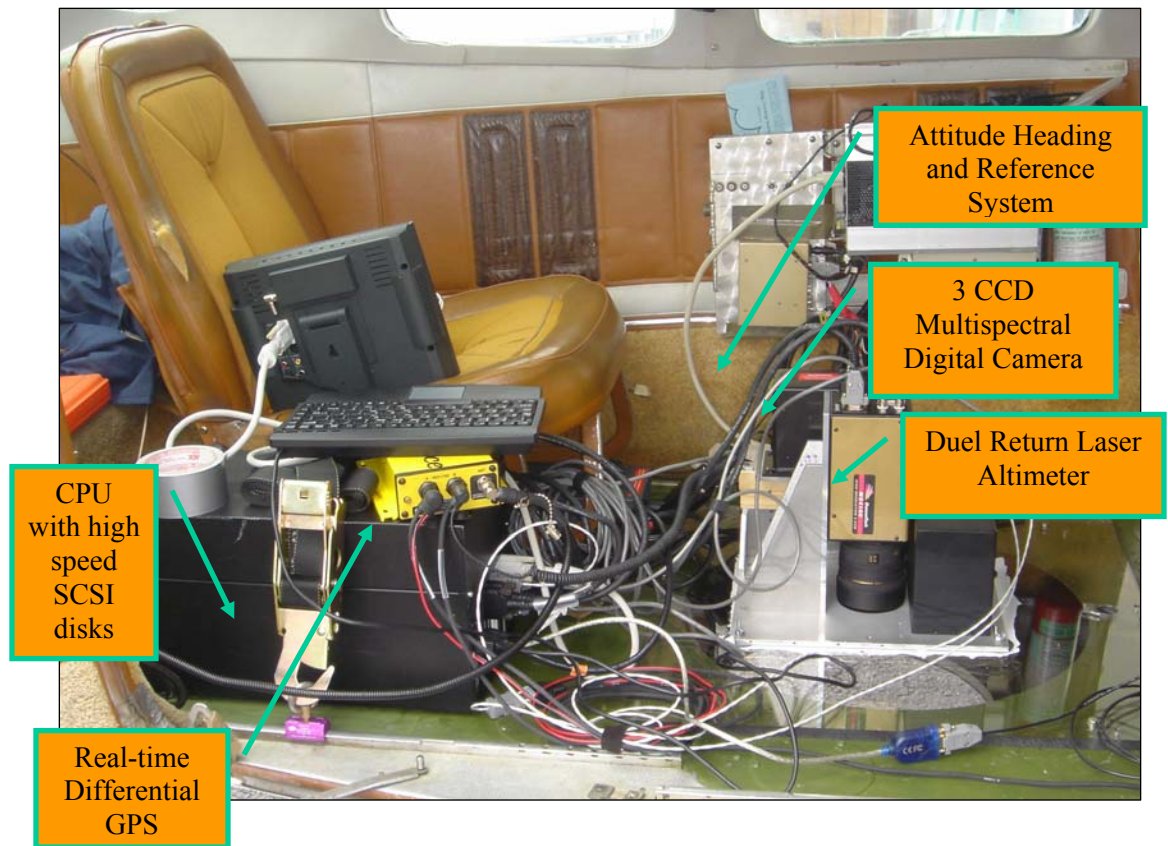
(*Figure 5*): Image of the AIMS-1 sensor with labeled components.

Initial examination of adelgid infestation took place through viewing

images captured by the AIMS-1 sensor (Figure 5) in April of 2004, during leaf

senescence of the hardwood stands. The AIMS-1 sensor was developed in the

GeoProcessing Lab at Mount Holyoke College (Millette & Hayward, 2005), and

provides a variety of remotely sensed data useful in forest management activities.

AIMS-1 captures images in four spectral bands at 0.40-0.52μ, 0.54-0.59μ, 0.64-

0.69μ, and 0.78-0.84μ in order to be comparable with Landsat TM data. The

Charged Couple Device (CCD) can capture 8-bit (256 color variations through

each band) data in the four spectral bands, or 10-bit (1024 color variations) data in any three channel combination. The CCD captures up to 10 frames a second, with a 14mm lens. In this study, the spatial resolution of the imagery is 25 cm on average.

In addition to the band information, the sensor contains a Trimble AgGPS 132 12 channel differential GPS receiver, capable of instantaneously locating the aircraft's position for georectification. The GPS information can also be used to develop flight lines in a GIS and provide the pilot with navigation directions. Flight lines are displayed on a 10.4 inch heads-up display that allows the pilot to choose background images such as topographic maps, navigation charts, and digital orthophotos.

Positional information, in addition to the plane's orientation, pitch rate, roll rate, yaw rate, heading rate, and bank and elevation are key components within the sensor. These measurements are acquired by the Attitude and Heading Reference System (AHRS), which records data 71 times a second. Accuracy of this sensor component is approximately ±0.01° in attitude and ±0.1° in heading.

A profiling laser rangefinder (LIDAR) firing 240 times a second is used to measure the height of the aircraft during flight. It does this by recording the time-of-flight (TOF) of a 30ns laser for the first group of reflected photons and the last group of reflected photons. The first group represents those objects within the closest range of the airplane, and the last group measures objects with the farthest range (Millette & Hayward, 2005).

Data

Two sets of data were used in this study. The primary source of imagery was captured in April of 2004 in tri-band 8-bit format. This information provided 256 quantized levels of color information through the near infrared, red, and green bands. Tests performed later in the study used images captured in October of 2004 in tri-band 10-bit format. This provided 1024 quantized levels of information through the near infrared, red, and green bands. The location of 10-bit tests differed from the plots used in the 8-bit tests.

Data Processing

A geographic information system (GIS) map of the Quabbin (Figure 6) with marked vegetation types was created previous to this project. The Division of Water Supply Protection under the direction of the Massachusetts Department of Conservation and Recreation, monitors stand health by taking forest metrics on individual trees in approximately 420 fifth-acre plots located throughout the watershed. Plot notes from 2000 enabled foresters to give accurate information as to where damaged stands were located, and pass that information to me.

Through the use of GIS software, the flight line of the plane on which the sensor was mounted and the corresponding images taken were added to the preexisting vegetation map. The Global Position Sensor device (GPS) located within the AIMS-1 sensor array provided position information once every second. This enabled each image to have precise location information, making

georectification possible. Map projections used for all operations in this study

were georeferenced in NAD (North American Datum) 1983, state plane,

Massachusetts mainland, meters. Georeferencing is fundamental in order to

accurately locate any map feature.
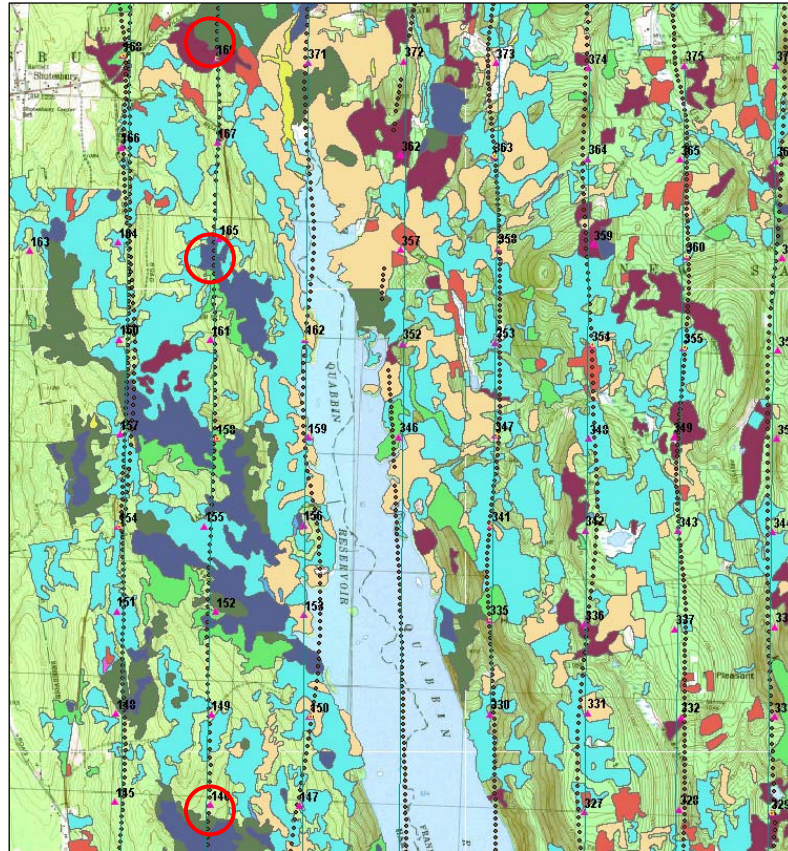
(*Figure 6*): A GIS Map of a portion of the Quabbin. Colored polygons represent different
vegetation types within the forest. Also visible on this image are continuous forest index
(CFI) plots represented by small pink triangles with numerical values next to them.
Foresters visit these plots to monitor stand development. The last recorded visit by the
DWSP was in 2000 and it was then that foresters noted where damaged hemlocks were
located. The vertical dots represent the flight and the corresponding frames taken as the
plane traversed the Quabbin. Lastly, the circled areas are the locations of the three
primary plots used in this study.

The georeferenced images needed to be examined to discern if it was

possible to visually determine infestation (Figure 7). Three plots, 146, 165, and

169, located along the same flight line were identified as damaged using the information provided by foresters working within the Quabbin. Discerning individual hemlock health will be described in the next section titled Visual Analysis. These plots have assigned numbers because they coordinate with the continuous forest index (CFI) plots that the Division of Water Supply Protection uses to monitor stand health. Having the stands located on the same flight line normalized illumination effects, minimizing different interpretations of tree damage. Interactions between forest canopy and incident sunlight can result in a variety of different spectral responses that either aid or hinder the identification of tree crowns (Lamar et al, 2005). Keeping incident sunlight relatively homogenous for all three stands minimized the errors due to illumination differences. These sites were comprised mostly of hemlock, with Plot 169 containing the most hardwoods of the three plots. Alternative sites were heavily composed of other vegetation types such as white pines, red pines, and spruce, which would have added error into the tree identification process, and were not chosen for that reason.
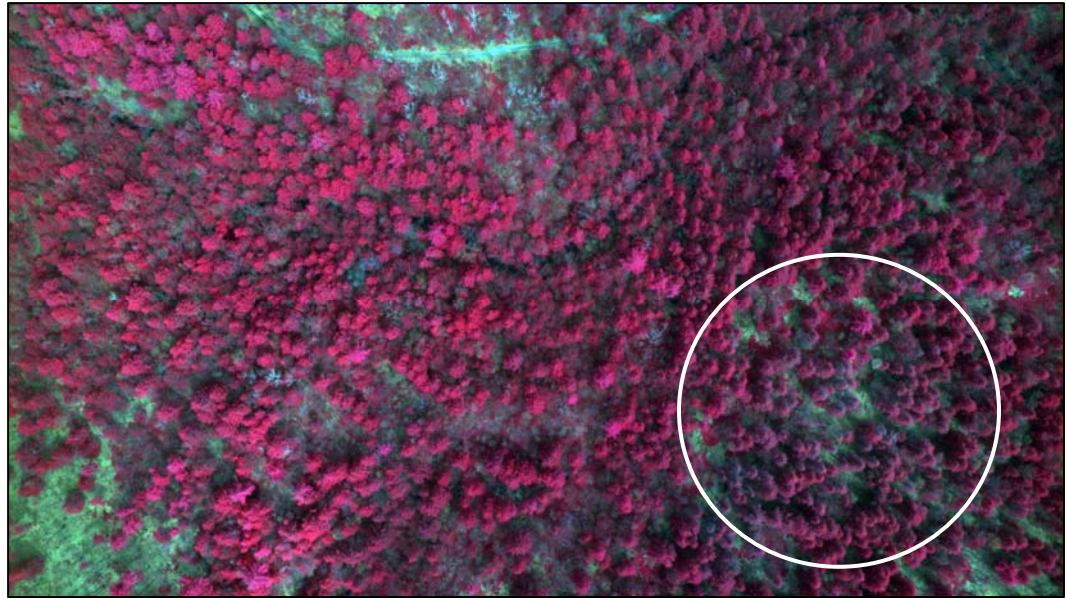
(*Figure 7*): Located three frames below CFI plot 146, this image shows woolly adelgid damage. Notice the different shading of the trees, and their drastically darker appearance. This is in part due to hill aspect, but it also shows the different color of damaged trees.

After identifying sites that looked to be infected upon primary interpretation, it was necessary to build stereo blockfiles in ERDAS image analysis software. A stereo blockfile is a set of images that are georeferenced to one another, and a control image with a ground reference, through the creation of tie points linking corresponding places in images. Building a blockfile is necessary in order to orient the image to the ground for truth data collection. When creating the blockfile it is important to have the lowest amount of error possible, so when ground referencing of the data occurs, the trees are close to their projected locations. The total Image Weight RMS Error for Plots 146, 165, and 169 are 0.965, 0.592, and 0.496 meters respectively. Additionally, by building a blockfile the image can be viewed in three dimensions. To accomplish this, two images are projected at opposing angles to each other. Using polarized classes and

a specialized monitor, the two images then appear in 3-D, much like the technology used for movies. Stereo viewing allows for a closer look at damage upon the branches of trees because it becomes possible to zoom towards the tree trunks and see where the remaining needles producing chlorophyll are located in relation to the base of the tree.

Once the blockfiles for each plot were finished, individual tree polygon measurements were taken using ArcGIS. In ArcGIS 2-dimensional shapefiles allow the examiner to zoom to the affected area of the image and capture the exact pixels for each polygon. Initially, two vegetation classes were delineated, Healthy_Hemlocks and Damaged_Hemlocks and were then digitally processed. These polygons were supposed to highlight the measured difference in the density of vigorous needles compared to the density of needles no longer producing chlorophyll. Separate GIS shapefiles were created for each damage classification in each plot, but the names were constant so data can be combined in the future (Figure 8). Ground-truth data, while important, was not addressed at this juncture.
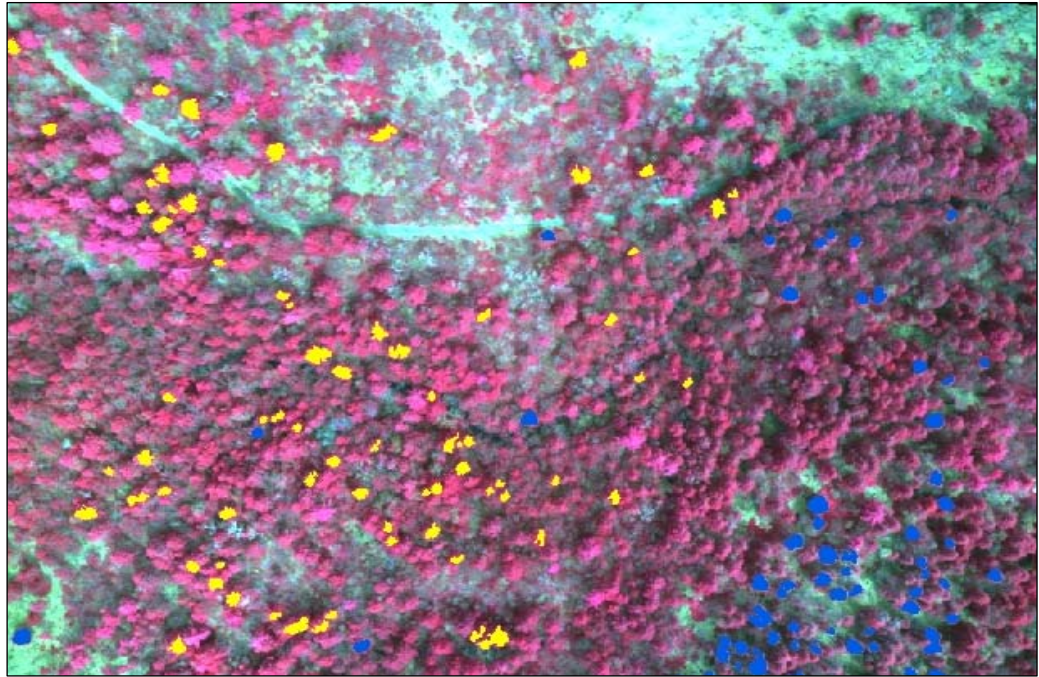
(*Figure 8*): Image showing an identified damaged plot, 146, and vector polygons on top of each tree labeled as healthy or damaged. Yellow polygons represent damaged hemlocks and blue represent healthy hemlocks.

Visual Analysis

An important part of this project involved developing an understanding of hemlock shape characteristics within images. The hemlock typically has a circular or conical appearance, with a noticeable apex at the center, depending upon the angle of the image. In Figure 9 below, the arrow points to the damaged hemlock's apex, giving a representation of the standard pattern to look for when identifying hemlocks, damaged or healthy. The branch patterns generally show circular gaps in the trees' thick foliage. A representation of this pattern can be seen in Figure 10. This was seen more in healthy hemlocks, as damaged trees generally appeared to be very thin.
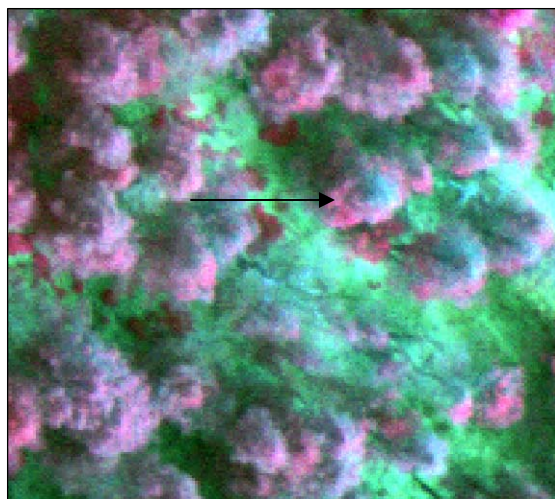
(*Figure 9*): Close up of damaged hemlocks.
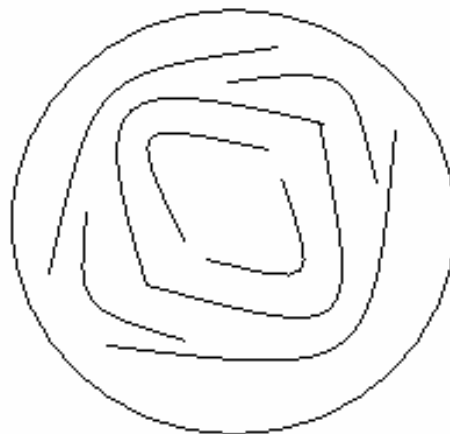
(*Figure 10*): View of hemlock from above.

Trees classified as damaged tended to be heavily infested. The adelgid initially feeds at the bottom of the tree moving upwards, and can be normally dispersed throughout the tree (Shields et al, 1995). The most noticeable pattern of damage was the ring of chlorophyll producing needles at the tops of and around the edges of the hemlocks. The dispersion of adelgid damage made trees nearest to death easier to identify, with those that were only beginning to be affected by the adelgid not as obvious. This in turn means that it was difficult to distinguish between differing stages of infestation, and lightly infested trees oftentimes were not included in the damaged classification. This gap in identification also created challenges when measuring spectral responses between each plot as there is great differentiation and the amounts of damage the trees were experiencing.

Accounting for these extra variables and becoming familiar with typical hemlock shapes was an important part of this study. Interpretation of the 10-bit data required examination when the hardwoods were in a leaf-on state, sometimes

shadowing hemlock branches. Without prior photo interpretation skills, these trees would have been impossible to identify.

Spectral Analysis

After defining trees within both feature classes, zonal attributes were run for all damage classifications through each of the three sensor bands. The attributes tested for each tree in the near infrared and red bands were maximum pixel value, minimum pixel value, mean pixel value, range of these values and the standard deviation. Statistics were performed using Microsoft Excel and SPSS. The mean pixel value is the primary focus because it quantifies the average spectral response for each individual tree. A comparison of maximum pixel values was completed for each plot and band; however it does not lend as much useful information because many of the infested hemlocks still are producing chlorophyll. This is a large problem for trees in the early stages of infestation, because much of the tree may still appear to be vigorous. Needles still producing chlorophyll will have the maximum pixel value, which isn't representative of actual hemlock health. Minimum pixel value is not useful because hemlock branches are often included within the polygons and those pixels would be counted as the minimums within both damage classifications. In this case, the minimum value would not be representative of the actual foliage, but of the branches.

The mean pixel values were then plotted on a graph against each tree location (this x-axis value had no significance) to discern if there was any difference between the two responses. These values were also used to test the statistical significance of the differences.

A t-test was performed upon the numerical data representing pixel values of the two samples of hemlocks: Damaged_Hemlocks and Healthy_Hemlocks. The t-test is the most robust way to determine statistical difference within a population. There are several assumptions needed for t-tests that the study fails to meet. With regards to random sampling, because I was discerning which trees I believed to be damaged and which I believed to be healthy, there was no random placement within the groups. The specific tree locations were dispersed throughout the plots, but this does not make the population truly random. In addition to there being no random sampling, there is no independent sampling. The distribution is normal, though, and the variances are homogenous.

After initial tests, it was noted that more than two vegetation classes would be needed to test the sensor's ability to detect spectral differences. The third plot, number 169, yielded different results from the first two plots, numbers 146 and 165. This anomaly forced the creation of more stringent tree classifications and future recognition of aspect differences. The new classifications are titled Damaged_Dark, Damaged_Light, Healthy_Dark and Healthy_Light.

Hemlocks are generally located upon hillsides, resulting in some light differentiation in images due to aspect. It should be noted that not all hillsides are shady for a large portion of the day; south or west facing slopes get more sun. Images from the three plots were all taken along the same flight line, so shadows from the sun would be approximately the same. Hill inclines differ in the three images though. What resulted were reflectance values of healthy trees being lower on the darker side of the image than the lighter side of the image, and the same being true for damaged tree. The dark and light extensions on the new classifications represent the dark and light sides of the images, accounting for the difference in hill elevation and incline. Figure 11 represents the same plot viewed in Figure 8, but there are now four damage classes present as vector layers on top of the image. The specificity of these classes will contribute to understanding the sensor's ability to detect adelgid damage through preservation of spectral differences, and will aid in future image segmentation by providing more detailed pixel values to classify damaged and healthy trees.

Also accounted for in these measurements was the individual shadow factor for trees where the shadows are too prevalent to accurately read what the tree's spectral signature should really be. In the case that a hemlock looked damaged, but there was a shadow on the tree, careful measurements were made in order to keep these pixels out of the data. This identification of shadow is separate from the dark and light sides of the image that were identified.
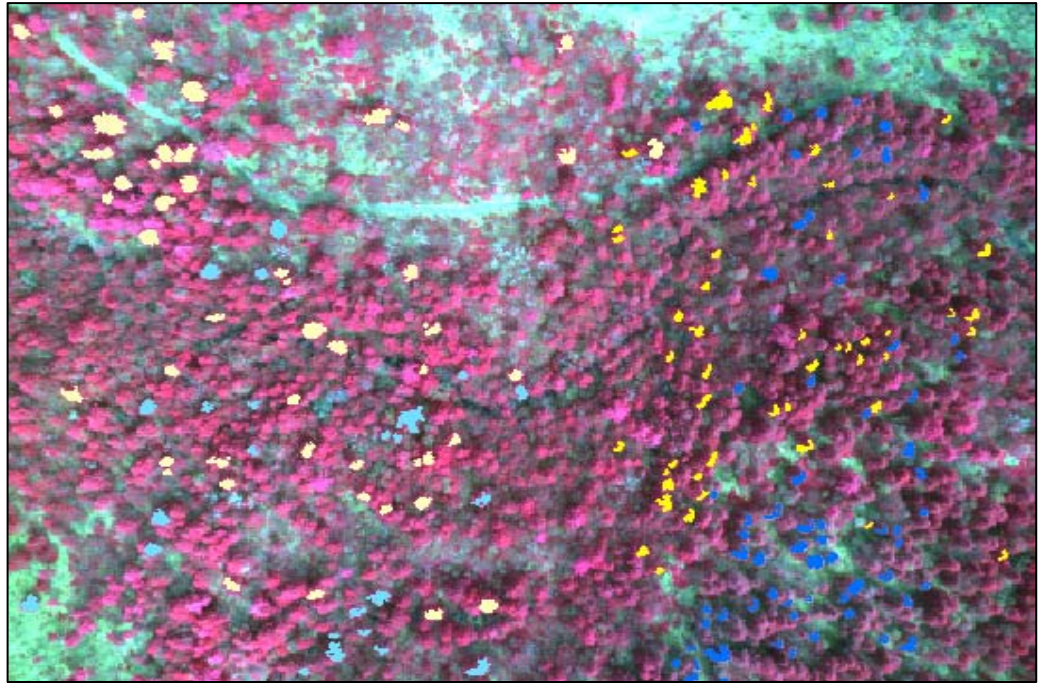
(*Figure 11*): Plot 146 with polygons separating two classes of damaged and healthy hemlocks, for a total of four different. The right side of the image is the darker side of the image, and the darker yellow and blue represent tree classifications Damaged_Dark (blue) and Healthy_Dark (yellow). On the lighter side of the image, the same colors were used for each damage classification.

The next step was to test the spectral differences using vegetation indices. After creating the blockfiles, all of the referenced images were appended together to create a continuous image scene that included a larger area than each of the images provided alone. Creating a blockfile was also necessary to create a mosaic image. The purpose of the vegetation index is to stabilize internal effects such as canopy background, soil variations, and differences in senesced or woody vegetation that can skew results within a CIR or RGB combination image. The first vegetation index completed was the normalized difference vegetation index (NDVI), which separates the information in the red and near infrared band. This vegetation index contrasts the absorption properties in the red band against the

high reflectance of plants in the NIR (Elvidge & Zhikang et al, 1995). In a

damaged site, the chlorophyll absorption should be low relative to the healthy

plants, and that difference should appear in the index results. While the NDVI is

the most common index tested when examining chlorophyll levels, other indices

also relay similar information. Three indices were run in order to test which index

provided the most information about the sensor's ability to detect adelgid damage

and hemlock health (Bonneau et al, 1999b). Equations of all indexes used in this

study are listed in Table 1. Each relays different information about atmospheric

conditions utilizing the second and third bands, which hold the most information

concerning vegetation. Their functions can be found within the third column of

the table.

Index	Formula	Assesses
Normalized Difference Vegetation Index (NDVI)	$\dfrac{(NIR - Red)}{(NIR + Red)}$	Chlorophyll content and energy absorption.
Transform Normalized Difference Vegetation Index (TNDVI)	$\dfrac{\sqrt{(NIR - Red)} = + 0.5}{\sqrt{(NIR + Red)}}$	Chlorophyll content with a stabilized variance
Soil Adjusted Vegetation Index (SAVI)	$\dfrac{(1+L)\ (Band\ 3 - Band\ 2)}{NIR + Red + L}$	Minimize soil brightness if moisture is present.

(*Table 1*) The three vegetation indexes performed on the numerical data. There are hundreds more vegetation indexes that have been created, however many utilize hyperspectral data, which differs from the broadband data used in this study. Formulas found in Jensen, (1996).

Spatial Analysis

Another test performed in this study attempted to quantify the amount of adelgid damage within a stand. Foresters working within the Quabbin care less about the damage stage of individual trees and more about the percentage of damage within a stand. Forestry practices warrant the salvaging of a stand that is over 50% damaged. The logic underlying this practice is that, once a hemlock is infested, it cannot be saved, and with over 50% damage it is more cost effective to harvest the stand and acquire revenue from the sale of the timber (DWSP, 2004). In order to perform this test, a subset of Plot 165 was digitized as an entire hemlock stand. It falls within the boundaries of a much larger hemlock stand and the flight lines don't cover the entirety of the stand, so images are not available to examine the entire plot. All hemlocks within the subset of Plot 165 were digitized. The number of damaged trees was then divided by this total number in order to test if there was more than 50% stand damage.

The purpose of the subset test was to see if an automated process could identify damage more efficiently than manual delineation of hemlocks (the method used in this study), or ground truthing. Using spectral signatures of the healthy hemlocks and damaged hemlocks, a supervised classification was performed in order to generate images to visually display the homogeneity and heterogeneity of spectral responses within both vegetation classes. Because each pixel is tested and placed within a certain signature category, the chances that objects will appear whole after classification are somewhat slim.

10-Bit Data Analysis

It was thought that if 8-bit data could not provide information about the sensor's ability to detect spectral differences, then 10-bit data might be used instead. Images taken in 10-bit measurements were captured in October of 2004, before senescence of the hardwoods. This meant that the image data varied greatly from the spring data used in the rest of the study. Additionally, the image location is different in the 10-bit data, even though it is still located in the Quabbin. While the comparisons seem different because of the time at which images were taken, it is important to understand the sensor's functionality within a leaf on state as well. Hemlocks show damage in October like they do in March, and it is this health information that we are concerned about in the study.

RESULTS

Question 1: *Will infested hemlocks have statistically different maximum and mean spectral signatures when compared with healthy hemlocks?*

Plot 146: Band 1 is the near infrared band, which provides information about chlorophyll production within vegetation. The graph below (Figure 12) displays the results for the comparison of mean pixel values for damaged and healthy hemlocks in Plot 146, Band 1. All pixel values are taken from individual digitized polygons, which contain more than 1 pixel. Visually there is clear differentiation between the trees classified as damaged (blue) and those classified as healthy (yellow). The mean pixel values of healthy hemlocks range significantly higher than the mean pixel values of the damaged hemlocks.

Mean Pixel Values for Hemlocks in Plot 146 through Band 1
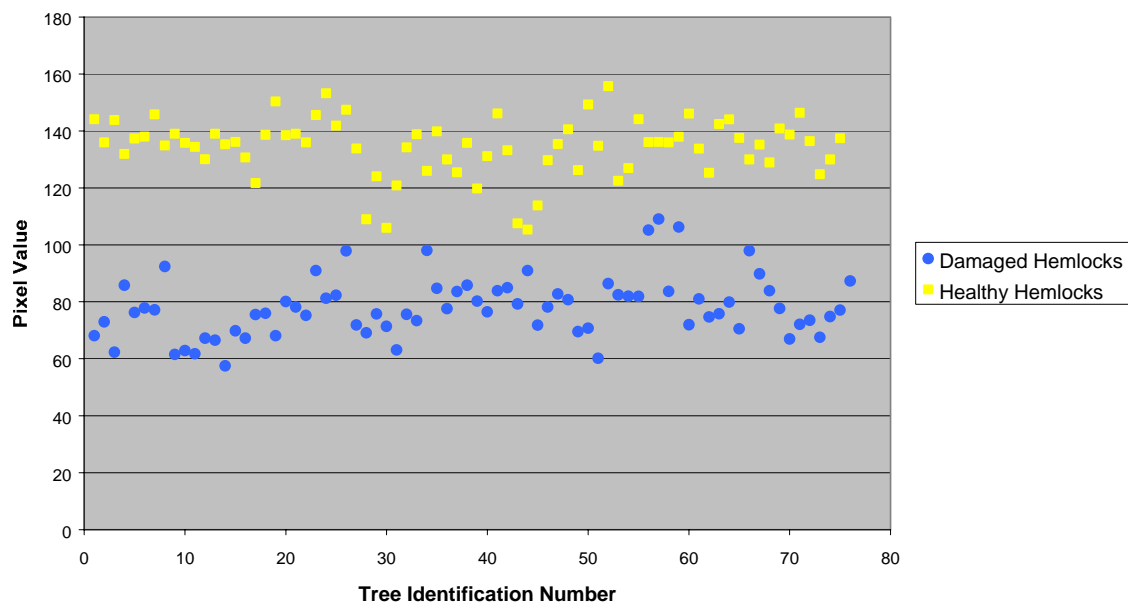
(*Figure 12*): The above graph represents the mean pixel values in Band 1 for each measured tree in Plot 146. While there is some variability within individual trees, the mean values appear to be very different.

The graphical representations show clear separation of hemlock health classes, but statistical verification is still necessary as evidentiary proof of actual difference. Group statistics and t-test results for the mean pixel values in band 1 are listed in Table 2 (Appendix A). The t-statistic is 33.124 which is stronger than the t-critical 1.645 for the number of samples within this test with a p-value of .0001.

The maximum pixel values of the two hemlock classes show similar trends when compared with the mean pixel values (Figure 13), with clear differentiation between the maximum pixel values of healthy and damaged

hemlocks. The difference is not as defined as that of the mean pixel values, but it is still apparent and significant.

Maximum Pixel Values for Hemlocks in Plot 146 through Band 1
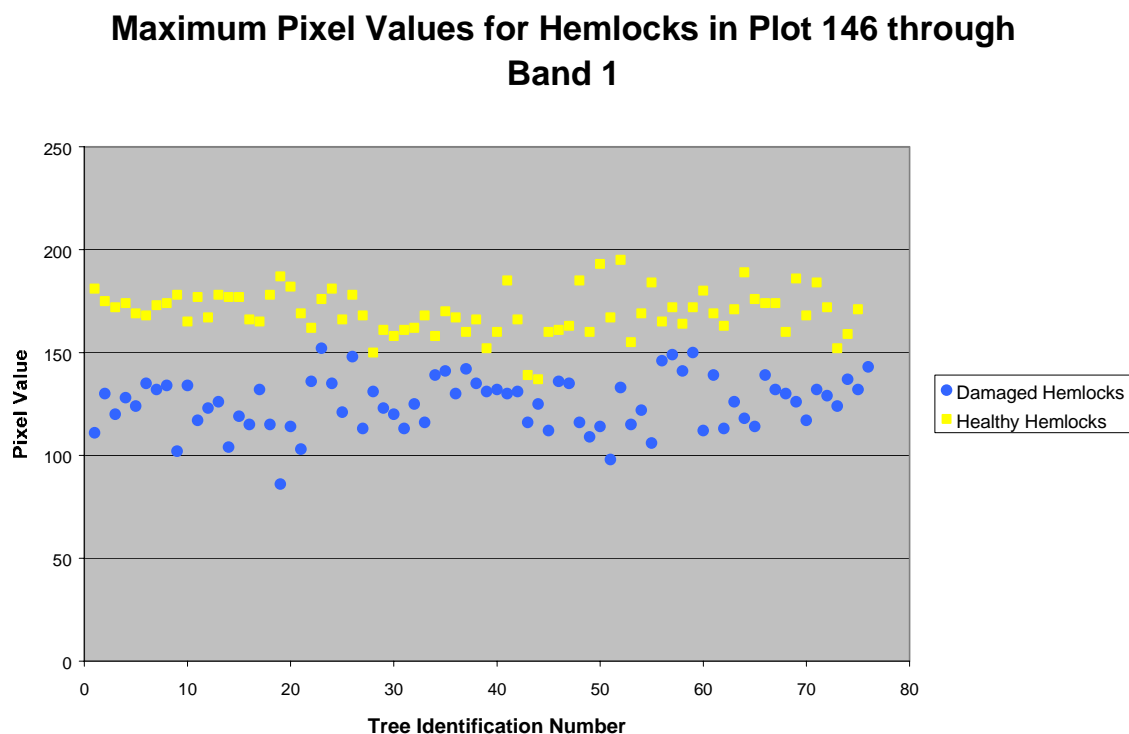

(*Figure 13*): The above graph represents the maximum pixel values in Band 1 for each measured tree in Plot 146. The variability within individual trees is noticeable, but the maximum values are still different.

Table 3 (Appendix A) shows the results of a t-test on the maximum pixel values in Plot 146, Band 1. The t-statistic is 22.55 which is stronger than the t-critical of 1.645 for the number of samples within this test with a p-value of .0001. Again, this shows that there are statistically different responses between the hemlocks within the damaged and healthy classes.

In Figure 14, the mean pixel values for Hemlocks are displayed for Band 2, Plot 146. While the damaged hemlocks do have higher reflectance values for

the most part, it is clear from visual interpretation that a trend does not exist. This

does not preclude the test from actual statistical significance.
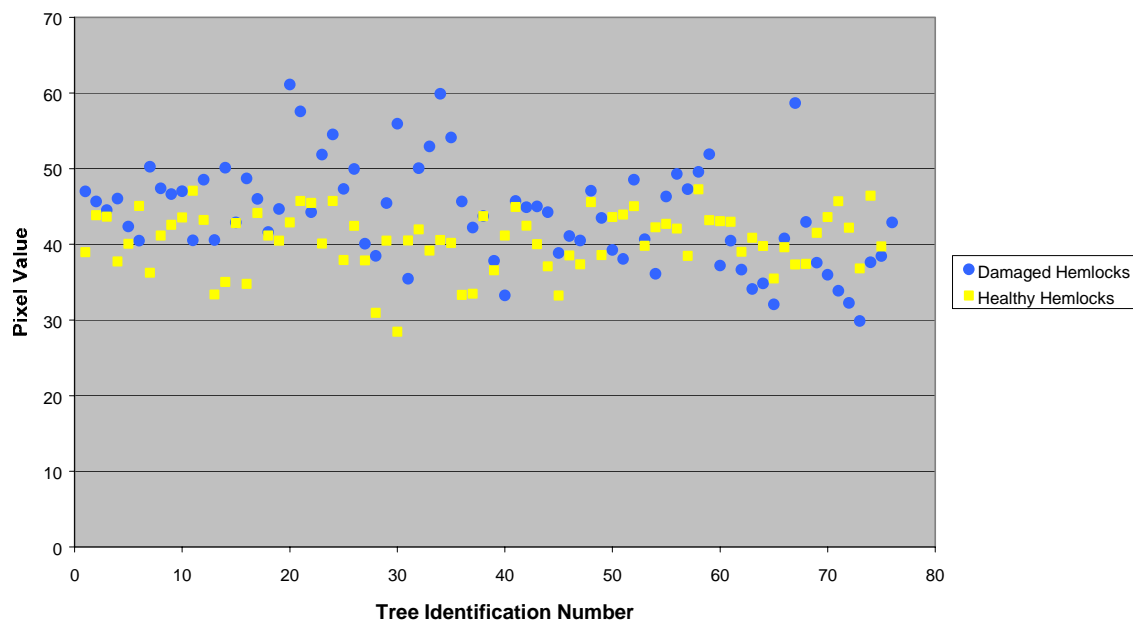
(*Figure 14*): The above graph represents the mean pixel values in Band 2 for each measured tree in Plot 146.

Statistics were computed using the mean pixel values within Band 2 for

damaged and healthy hemlocks Table 4 (Appendix A). There is noticeable

variation between the maximum values of damaged and healthy hemlocks within

Band 2. The t-statistic is 3.871which is stronger than the t-critical of 1.645 for the

number of samples within this test with a p-value of .0001. Statistics prove that

there is a difference between the population.

Maximum Pixel Values for Hemlocks in Plot 146 through Band 2
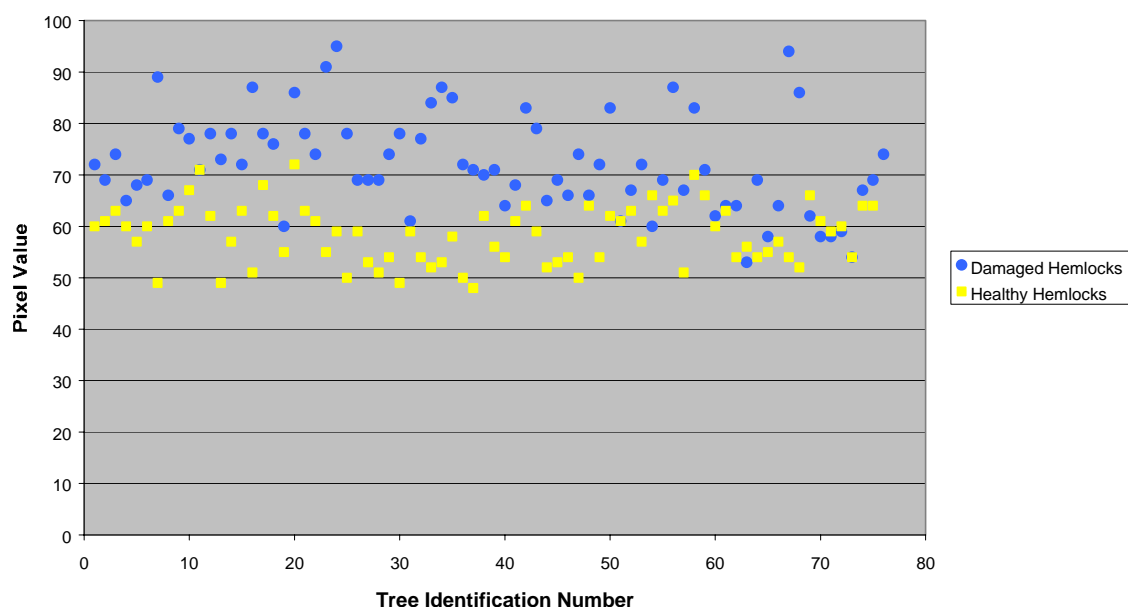
(*Figure 15*): The above graph represents the maximum pixel values in Band 2 for each measured tree in Plot 146. Obvious is the trend where infested hemlocks reflect more light than healthy hemlocks.

The results for this t-test can be seen in Table 5 (Appendix A). The t-statistic is 10.82 which is stronger than the t-critical of 1.645 for the number of samples within this test with a p-value of .0001.

Plot 165: The second plot of tree measurements was taken near CFI 165, and shows similar results to Plot 146. In Figure 16, data from Band 1 is presented. There appears to be higher reflectance means for healthy hemlocks (yellow) than for damaged hemlocks (blue) (Table 6, Appendix A). The t-statistic is 19.28 which is stronger than the t-critical of 1.645 for the number of samples within this test with a p-value of .0001.

Mean Pixel Values for Hemlocks in Plot 165 through Band 1
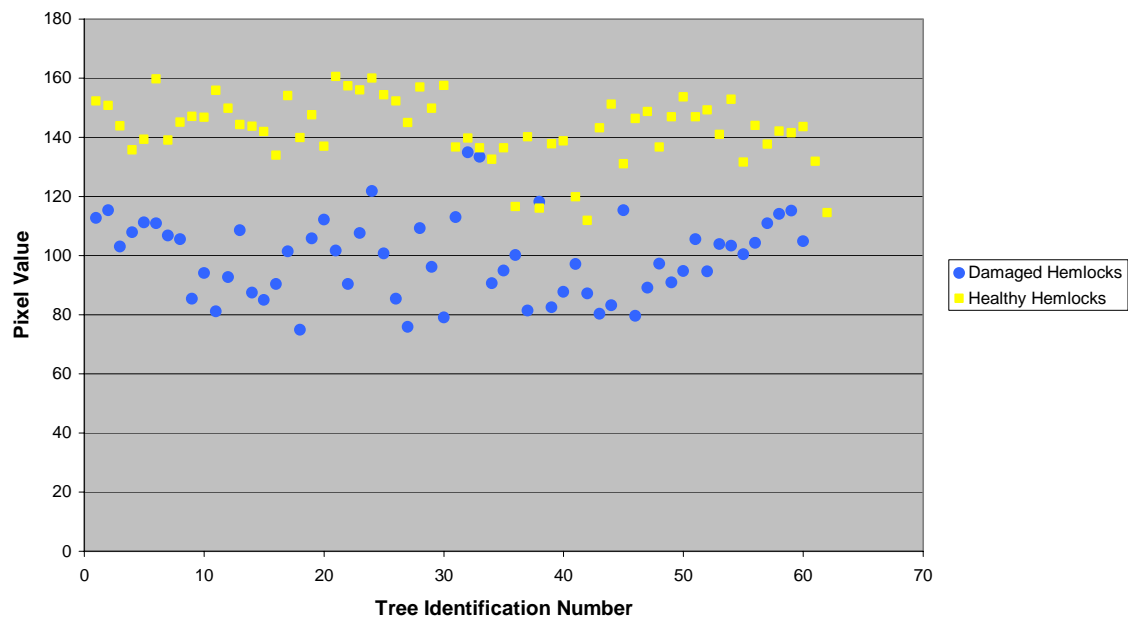
(*Figure 16*): The above graph represents the mean pixel values in Band 1 for each measured tree in Plot 165. Notice the extreme difference in the damaged hemlocks, which are not reflecting light, and the healthy hemlocks, which are reflecting normal chlorophyll production.

When looking at the maximum pixel values for damaged and healthy hemlocks in Plot 165 Band 1, visual differences in the reflectance patterns of the two groups become apparent (Figure 17). The standard deviations are similar. The t-statistic is 14.68 which is stronger than the t-critical of 1.645 for the number of samples within this test with a p-value of .0001.

(*Figure 17*): The above graph represents the maximum pixel values in Band 1 for each measured tree in Plot 165. In band 1, healthy vegetation should reflect more light and have a higher pixel value.

Figure 18 is the graphic representation of the mean pixel values for Plot 165 in band two. While there is statistical difference between the mean pixel values for the damage classes, this relates to the extreme values within the damaged classification (Figure 18). Reflectance values for healthy hemlocks appear to be homogenous, generally ranging within a certain boundary of absorption. T-statistic is 8.1 which is stronger than the t-critical of 1.645 for the number of samples within this test with a p-value of .0001.

Mean Pixel Values for Hemlocks in Plot 165 through Band 2

(*Figure 18*): The above graph represents the mean pixel values in Band 2 for each measured tree in Plot 146.

Figure 19 is the graphic representation of the maximum pixel values in Plot 165. There is great amount of heterogeneity between the spectral signatures, but there is still statistical difference within the data. The t-statistic is 17.8 which is stronger than the t-critical of 1.645 for the number of samples within this test with a p-value of .0001. Statistics show that there is a difference between the population.
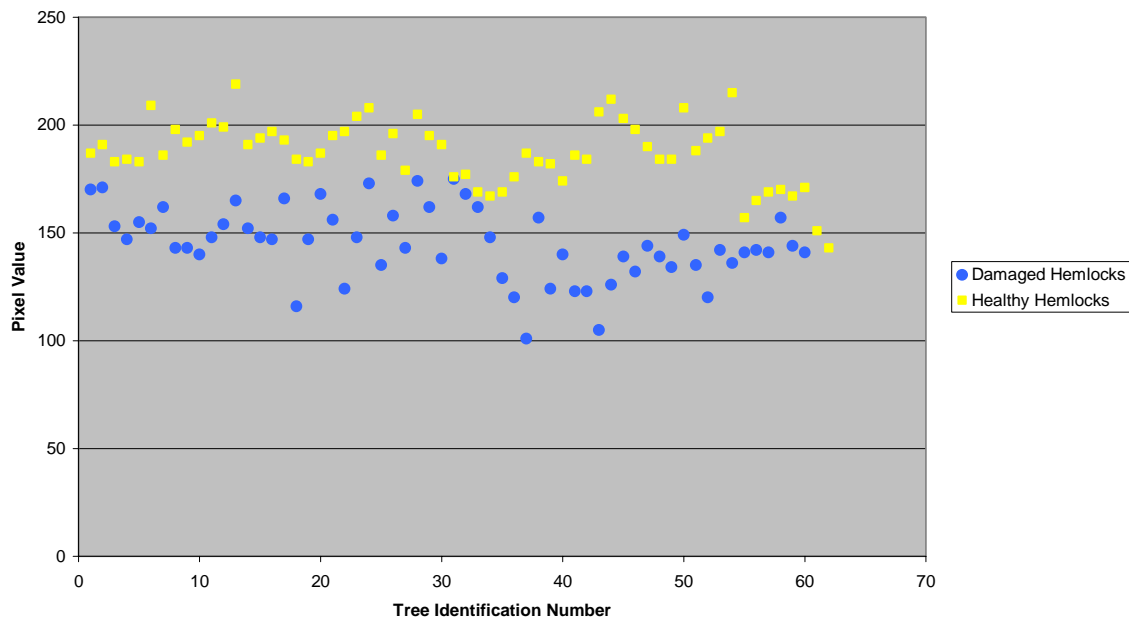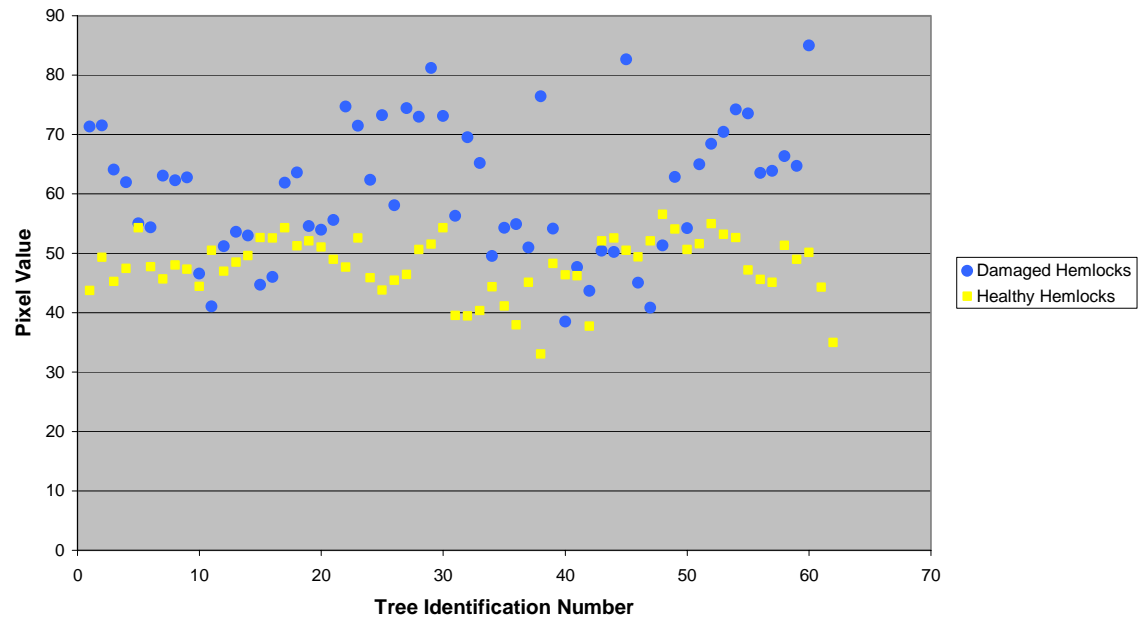
Maximum Pixel Values for Hemlocks in Plot 165 through Band 2

(*Figure 19*): The above graph represents the maximum pixel values in Band 2 for each measured tree in Plot 165. Signature responses show no statistical differences.

Plot 169: Within Plot 169 there are major discrepancies in the data, and there is no pattern with regards to the pixel reflectance values. Figures 20 and 21 show the mean pixel values and maximum pixel values in Band 1 for Plot 169. This data were surprising because the other plots mirrored each other in their results.

Upon closer inspection, an inconsistency with regards to the sampling method was noticed. Within the lighter side of the image there were not as many healthy hemlocks, and there were relatively no damaged hemlocks—the lighter side of the image was composed mostly of white pines. This means that the majority of tree measurements were taken within the darker side of the image.

Another inconsistency in Plot 169 was its relative heterogeneity when compared to Plots 146 and 165. Both of those plots were homogenous hemlock plots with very few pines and even fewer hardwoods. While Plot 169 is still primarily comprised by hemlock, the presence of hardwoods is much greater when compared to the homogeneity within the other plots. These two major differences account for some of the dissimilarities in data, and forced me to create another method for testing the sensors preservation of spectral differentiation.
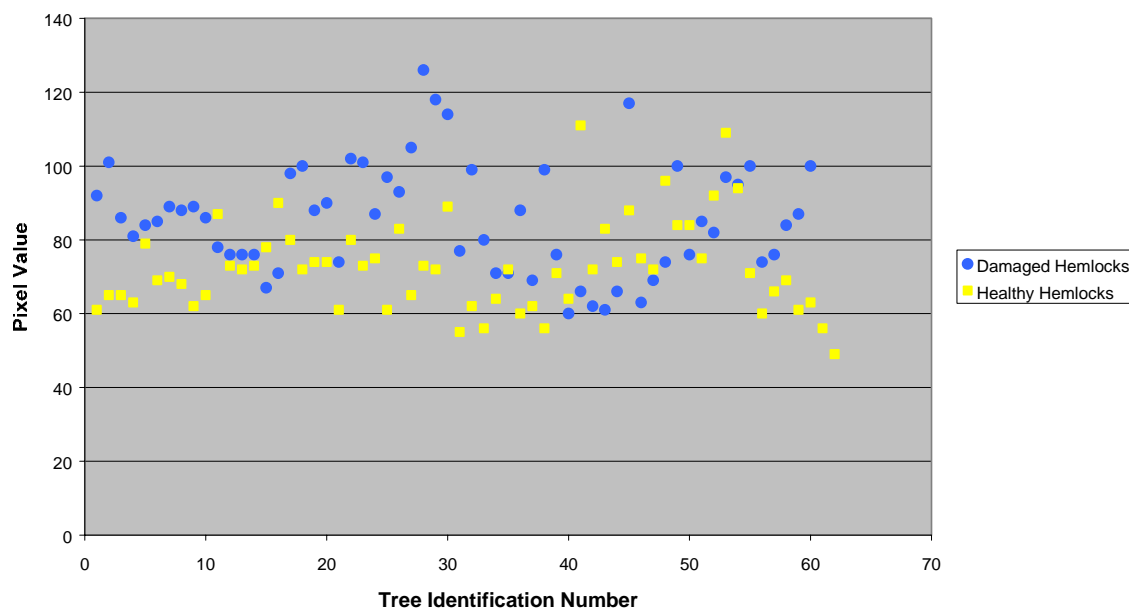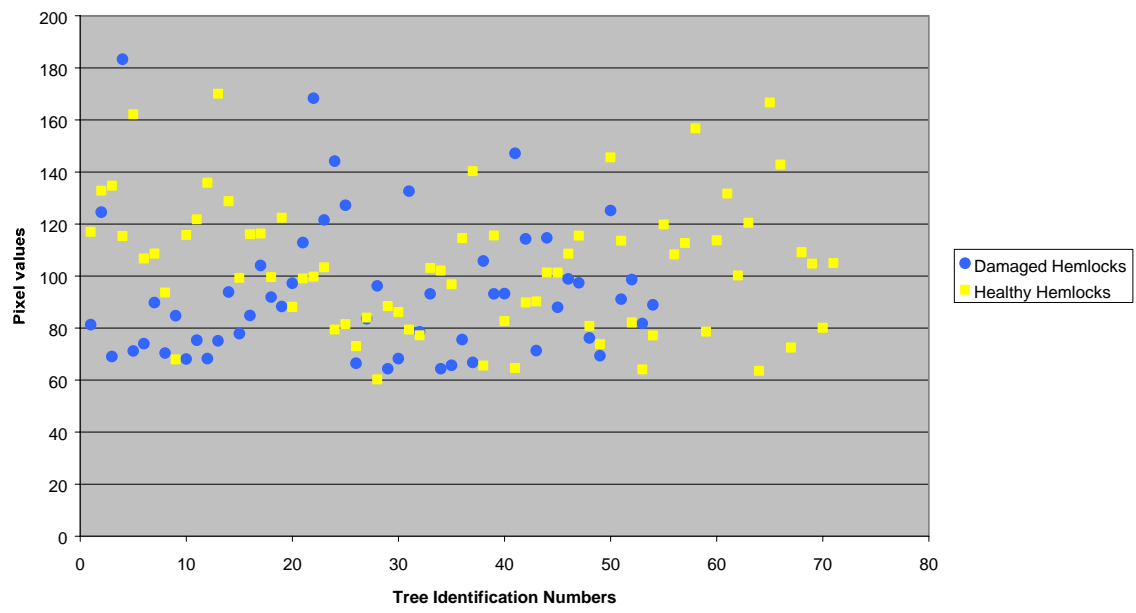
Mean Pixel values for Hemlocks in Plot 169 through Band 1

(*Figure 20*): The above graph represents the mean pixel values in Band 1 for each measured tree in Plot 169. Signature responses show no spectral differences, differing from the results of Plots 146 and 165.

Maximum Pixel Values for Hemlocks in Plot 169 through Band 1
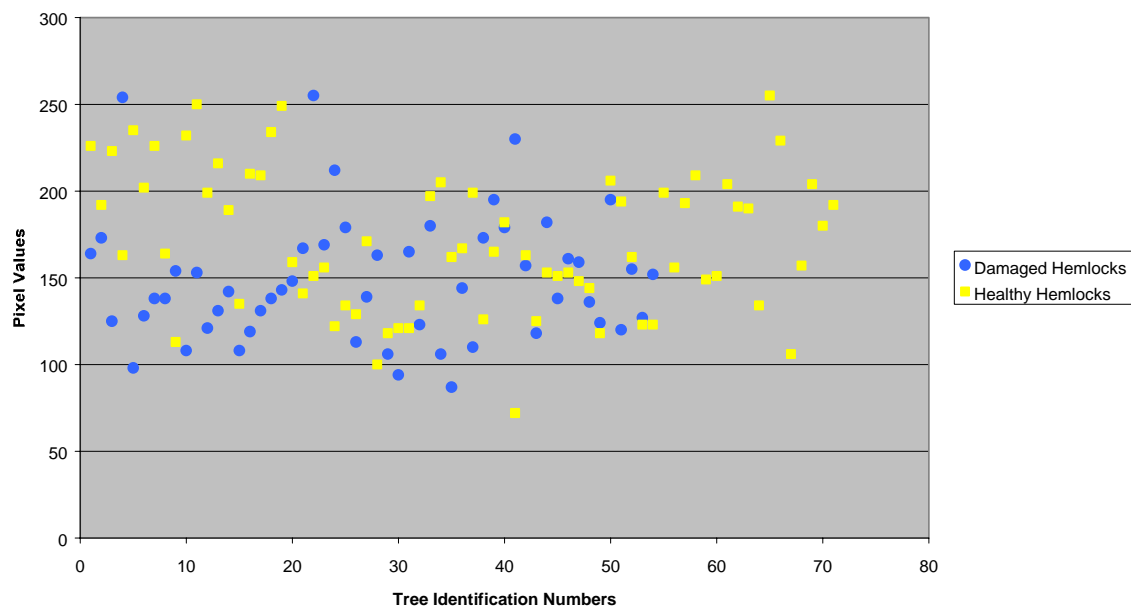
(*Figure 21*): The above graph represents the maximum pixel values in Band 1 for each measured tree in Plot 169. There is no difference between the damaged and healthy hemlock signature responses.

In order to correct for this inconsistency I created four vegetation classes instead of two. In these new vegetation classes, measurements of healthy and damaged hemlocks were taken from both sides of each mosaic image. This was based on photo interpretation, not ground truth identification.

Mean Reflectance Values All Measured Hemlocks in Three Plots on both Sides of the Image in Band 1
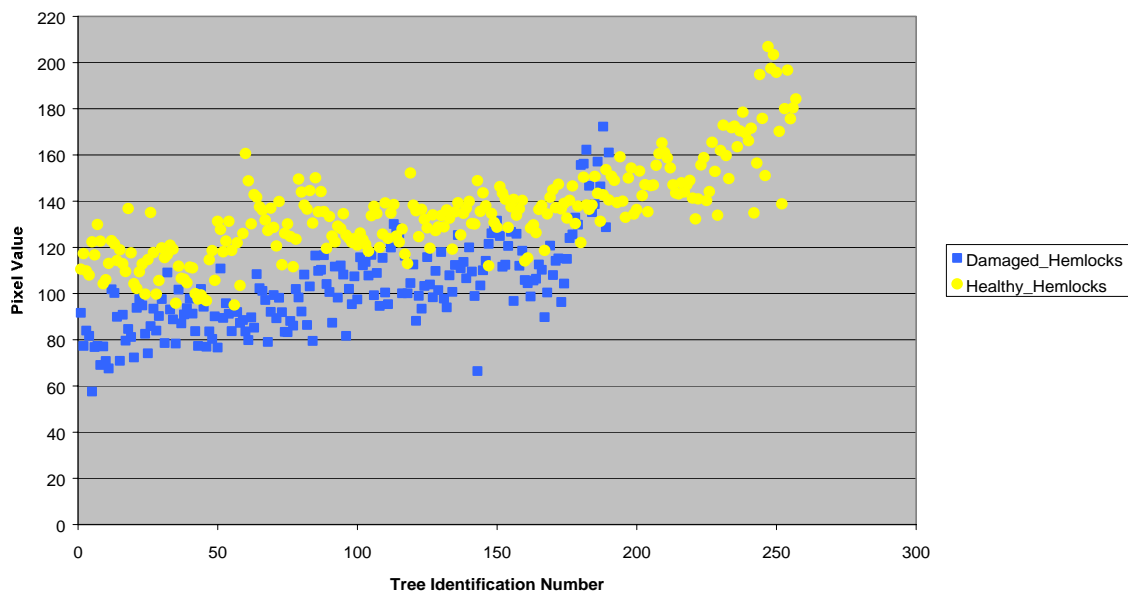
(*Figure 22*): Mean reflectance values of all measured trees within all three plots. Within the damage hemlocks class, trees identified as 1-117 are located on the dark sides of the images. Trees 118- 190 are located on the lighter sides of images. Within the healthy class, trees 1- 129 are located on the darker sides of images and trees 130- to 258 are on the light side of the image.

Figure 22 compares all of the measured trees, 447 in total, in Band 1. Results were displayed stand by stand before to highlight the differences in Plot 169 when compared to Plots 146 and 165. Band 1 is focused upon because the infrared band is regarded as the most informative concerning chlorophyll vigor. Statistics for Band 2 provide little consistent information concerning difference within damage classes, so tests were not completed within that band.

Figure 22 shows expected trends with damaged vegetation having a lower reflectance value in the near infrared channel. There is a less pronounced difference between the two classes when compared to Figures 12 and 16, but

these results mirror those figures. It should also be noted that the spectral

responses within the trees numbered 170-190 of the Damaged_Hemlocks

classification generally range higher than the rest of the damaged trees.

In addition to four defined spectral classes, more careful examination of

each tree leads to the most accurate pixel responses available for each polygon.

An independent t-test was run utilizing all of the tree damage information. The t-

statistic of 17.19 which is stronger than the t-critical of 1.645 for the number of

samples within this test with a p-value of .0001. These tests show that there is a

statistical difference between the two vegetation classes. The results of this test

can be seen in full in Table 9 (Appendix A).

Question 2: *Which vegetation index will relay the most information concerning hemlock decline?*

One way to account for external parameters within image data sets is to use a vegetation index. The most common index used to test the reflective properties of the near infrared band is the NDVI. The primary focus in Figures 23-25 is the distribution of vegetation index values. The distribution of data shows the sensor's ability to detect pixel differences and the vegetation indexes capacity to normalize background noise.
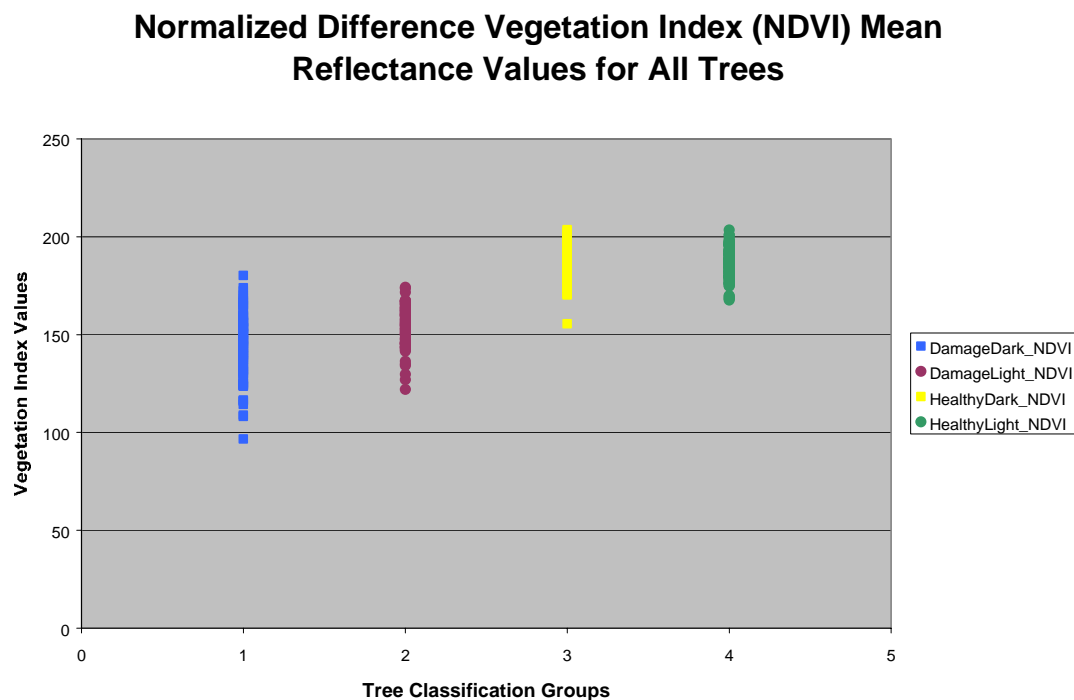
(*Figure 23*): Pixel variations of the four health classifications when performed in an NDVI.

Within Figure 23, the greatest amount of variation can be seen in the Damage_Dark classification. The patterns of reflection for the rest of the health classifications follow the expected pattern with both of the healthy vegetation

classes having the highest average pixel reflectance. The one anomaly is that there

are higher values within the Healthy_Dark classification than there are in the

Healthy_Light classification. The Healthy_Dark population should have a higher

reflectance than the damaged hemlocks and a slightly lower reflectance than the

Healthy_Light classification because of aspect interference.

Transform Normalized Difference Vegetation Index (TNDVI) Mean Reflectance Values for All Trees
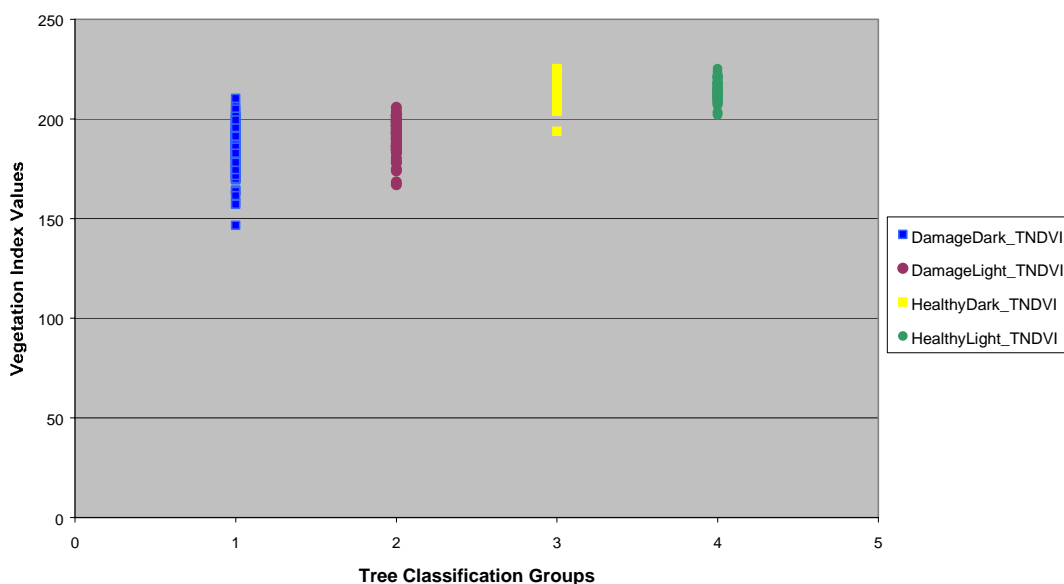
(*Figure 24*): Pixel variations of the four health classifications when performed in an TNDVI.

The variation trends are similar within the TNDIV (Figure 24) when

compared to the NDVI. The transform NDVI stabilizes the variance within the

data, and takes into account slope effects. While following the same trends as the

NDVI, there is less variation within the Damage_Dark classification. Especially

noticeable is the tight classification of the Healthy_Light population, showing the

similarity of the spectral signatures in this vegetation class. The narrow fit within

this health class, shows that the sensor is responding the way it is expected to.

Soil Adjusted Vegetation Index (SAVI) Mean Reflectance Values for All Trees
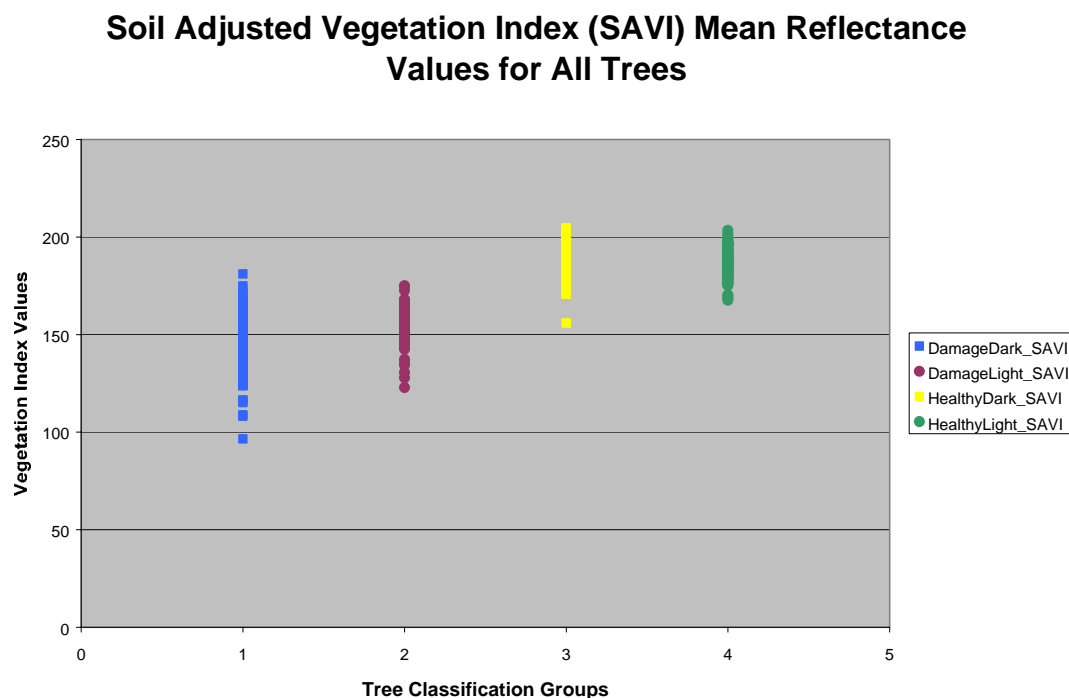
(*Figure 25*): Pixel variations of the four health classifications when performed in an SAVI.

The soil adjusted vegetation index (SAVI) (Figure 25) varies most within

the Damage_Dark classification, following the same trend as the other vegetation

indices. This relates to the fact that trees are in different stages of infestation.

Notice within the Healthy_Light classification the vegetation index values do not

appear to be as homogenous as the same population when tested using the

TNDVI. Image representations of the separate vegetation indices can be seen in

Figures 27-29 (Appendix A).

Question 3: *Can adelgid infestation be quantified by percentage of stand damage?*

The first method used to quantify the number of damaged trees present within the stand was to digitize each hemlock and assign it a health value. This was performed on a subset within Plot 165. Of the 223 hemlocks digitized, healthy trees comprised 74% (165 trees) and damaged trees comprised 26% (58 trees). This stand would not warrant clearing, as over 50% of the stand is not damaged.

The ultimate goal is to automate this selection process, so a supervised classification was performed using signatures taken from these two health classifications. Aspect effects are minimal within the subset, so the only real shadow variables came from the trees themselves. The resulting image can be seen in Appendix A (Figure 30), with a table of each corresponding color and its actual reference within the image (Table 10). The supervised classification did not display two discernable vegetation classes. There was more variability within the damaged class, which was to be expected because of varying lengths of infestation. Ground cover was consistently classified as damaged hemlock in addition to the unhealthy hemlocks. There were also differences within the healthy classifications. The color green is representative of the white pines found in the image, along with hemlocks that had high reflectance values at their apexes. Several healthy hemlocks reflect red, but there only appears to be a slight difference between the blue and yellow classes when compared with the red class. These anomalies do not provide useful information about the health of each

individual tree. At this point, the spectral characteristics of the hemlocks are not

homogenous enough for reliable automated pixel-based classification.

Question 4: *If 8-bit data cannot provide information and or quantify woolly adelgid damage, can 10-bit data provide any additional information?*

Upon initial inspection, it was thought that the 10-bit data might yield additional information due to enhanced radiometric resolution and an increase in quantized information levels. As noted in the methods section, 10-bit imagery was taken before senescence, when hardwoods were still bearing their leaves. This made identifying hemlocks difficult since occasionally their branches were hidden by other trees or shadow, and that is not a problem experienced within the spring images used for most of the study.

When viewed more closely, it became apparent that hemlocks could be viewed within the imagery. Through photo interpretation, 76 hemlocks were identified and then separated based on whether they appeared to be healthy or damaged. An equal number of hemlocks appeared to be damaged and healthy, with noticeable color differences in the damaged classification on the trees' apexes. The same process completed to discern the spectral differences within the damaged and healthy classifications of the hardwood leaf senescence data, was used for the 10-bit data. Zonal attributes were run for each polygon and the means were focused upon in order to get a general sense of each tree's average reflectance. The graph in Figure 26 shows that there is no statistical difference between the two vegetation classes within the 10-bit imagery.
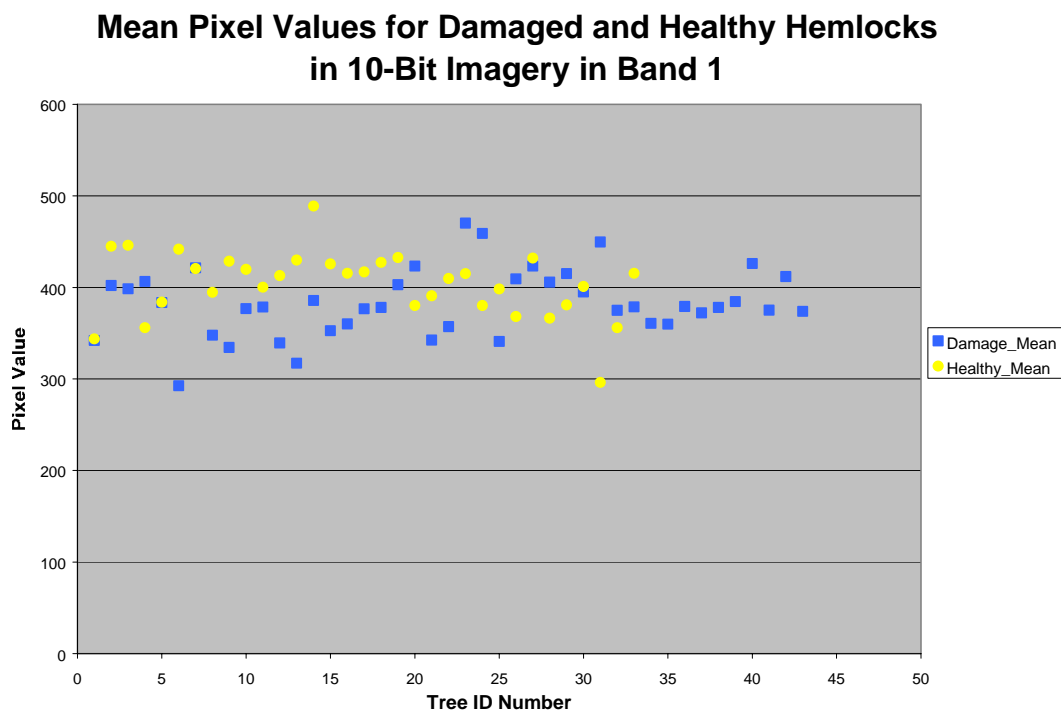
(*Figure 26*): Pixel values from 10-bit imagery to discern if vegetation classifications would be more homogenous.

DISCUSSION

Sources of Error and Variation

The identification of hemlocks posed a problem because of ground interferences and inexperience. Once the general characteristics of hemlock appearance within digital imagery were learned, this source of error decreased precipitously. To highlight an example of this kind of error, within the first data set some hemlocks digitized in Plot 169 were not actually hemlocks, but under-story vegetation mistaken as hemlocks. This factor could have played into the skewed results found within Plot 169 when compared to Plots 146 and 165. Two data sets were collected; the latter population with four vegetation classes was more accurate, with only hemlocks being digitized. This second set of data was collected in the same plots used in the first tests, with many of the same trees being digitized. The main differences of this second data set were the increase in the number of digitized trees, and four vegetation classes as compared to two vegetation classes.

The largest source of variation within the study was the trees. Measuring adelgid infestation was difficult because trees do not progress through damage stages at the same rate, making the variability of damage high. Within Plot 146, the majority of damaged trees were on the shady side of the slope, and were heavily impacted. Neither of the other two plots possessed such noticeable

damage. Additionally, in Plots 165 and 169, the aspect was not as severe and did not play as large a role in shadowing the stands. Within Plot 165, a number of trees were heavily impacted around the base and apex, but were still vigorous through most of the trees. These patterns are *typical* of trees within their first and third years of infestation (McClure, 1995), but it is impossible to discern the exact length of time a tree has been infected and level of damage without hyperspectral data.

In Plot 169, the classification of infestation was problematic because the trees were surrounded for the most part by senesced hardwoods. Comprising the majority of forests within the Northeast, the interference of hardwoods is a constant variable. The hardwood's branches often overlapped with the hemlocks skewing mean pixel values in both damage classifications. This was not a problem within the other plots, as they were relatively homogenous hemlock stands. Results in Plot 169 were different, even after the tests accounted for aspect and shadow interference.

All trees within the second set of data were classified correctly and although these trees identified as infected were damaged, some hemlocks were still producing new growth on the edges of their limbs. Zonal attributes therefore record these values. The variability within the damaged class is troubling, especially when compared to the consistency of the healthy hemlocks.

Examining the data graphically shows these trees falling either below or above the mean pixel value. The responses of healthy trees showed a much

stronger correlation throughout the plots when represented graphically. This is more representative of what the ideal spectral responses would be because of the homogeneity within the population.

Accounting for these factors, other than being mindful of them when processing the data and viewing graphic results, is difficult. It is important to include varying levels of damage in each populations in order to have a realistic representation of spectral differences within each damage class. The graphic results in Figures 12 and 16 show the variability of spectral responses for both damage classifications. At the same time, these heavily damaged trees skew the average and the results by drawing the average responses of each class further away from each other. The results end up showing statistically dissident differences without distinct separation of pixel values.

Comparison of Damage Using Two Classifications

The first method used to test the AIMS-1 sensor's ability to preserve spectral differentiation of hemlock woolly adelgid damage specified only two broad health classifications. External parameters such as tree shadow and aspect were not accounted for within the initial sample collection procedure. This introduced error into the results, showing pixel values within Plots 146 and 165 that varied greatly between tree health classifications. Without taking these parameters into account, misleading results showed that spectral differences could be detected by the AIMS-1 sensor and followed trends documented by (Jensen,

1996) and (Pontius, 2005). This differentiation between the means of the two damage classes in the infrared band can be seen in Figures 12 and 16. Plot 169, however, yielded different results, which can be seen in graph form in Figure 20. The mean pixel reflectance values test for Plot 169 showed no differentiation between healthy and infested hemlocks.

Band 2 is the red band in which healthy vegetation absorbs light. When a plant is under stress, chlorophyll production decreases, leading to an increase of reflectance in the red band. Figure 15 displays the maximum pixel values for damaged and healthy hemlocks in Band 2, Plot 146. In this band a healthy plant will have lower reflectance values in the red band than a damaged plant with diminished chlorophyll production levels. This is inversely related to the trends within Band 1 data, where reflectance values for healthy vegetation are very high.

Within Band 2, the red band, statistical outcomes varied. Statistical tests showed damage differentiation with great variability in most cases. Pixel difference was on average, only 3 pixels within the means test for Plot 146 (Table 4), but it was around 10 pixels for the maximum values test (Table 5). This trend exists because the red band is less sensitive to chlorophyll production when compared to the infrared band.

A primary goal in this study was to test the sensor's ability to preserve spectral differentiation, so these mixed results led to closer identification of differences within the images. This was done in order to determine why Plot 169 had such varying responses within both health classifications. Sampling methods

had remained constant through each of the plots, so it had to be some sort of

external interference that caused seemingly similar plots to have different results.

Comparison of Damage Using Four Specified Classifications

Differences in aspect were noticed and believed to be the cause of the

skewed results within Plot 169. Through examination of all three plots, the

conclusion was made that all images contained shadow differentiation due to

aspect. This was in addition to individual shadows within tight canopies.

Hemlocks typically prefer hillsides and riparian zones (Bonneau 1999a), so

interference because of aspect is to be expected within most hemlock stands.

To account for this variable, four vegetation classes were created. These

vegetation classes were more sensitive to the external parameters of shadow,

aspect and ground interference. Statistical tests were performed with the new data

set comprised of four vegetation classes. While the statistical fit was much tighter,

there were still very distinct trends in the data (Figure 22). The only band tested

was Band 1, because the information within the red band was so variable for the

other data sets, and didn't relay any consistent results.

Through having to use these specialized damage classes, some of the

sensitivities of the sensor became apparent. When capturing images, detection of

the damage was acute enough to warrant separate vegetation classifications within

the same health category. Additionally, these characteristics were relatively

homogenous between different image sets, showing that the sensor behaves

normally, and these results were normal throughout all captured images. This is important, as the AIMS-1, a broadband multispectral, CCD, digital camera has never been tested in identifying vegetation classifications. Previous work has been completed using broadband imagery from Landsat satellites to measure time change data, but the method attempted within this study was completely different.

10-Bit Imagery

It seemed somewhat incongruous that the 10-bit imagery provided no significant information to the study. With 1024 quantized levels, the potential of 10-bit imagery to detect pixel sensitivities seemed to be a sure thing. Part of the problem was the fact that the hardwoods were not in senescence like the 8-bit imagery. When hardwoods are in senescence the branches of infested hemlocks are visible, and can be captured during shapefile creation. Additionally, damage while apparent, was not as advanced as many of the hemlocks measured within the three original test plots. Capturing these branches during shapefile building was not possible in the 10-bit imagery.

Future Considerations

Vegetation classifications that are more defined can lead to image segmentation which will identify individual trees rather than pixels. This can provide foresters with the percentage of damage within any stand possessing hemlocks. The infestation of adelgid is a problem, and the more information

researchers have about their spread and the hemlock mortality rate, the easier it

will be to stem their spread.

.

CONCLUSION

These tests confirm that the AIMS-1 sensor is sensitive enough to preserve spectral difference within 8-bit data between infested hemlocks and healthy hemlocks in the near infrared band. Results for the red band are not conclusive, and generally it does not relay as much information about chlorophyll vigor. External parameters such as aspect and individual tree shadow must be accounted for when trying to characterize these damage classifications

The assessment of hemlock damage was possible because of the high spatial resolution within the data. At roughly 25cm, ground detail was visible and pronounced. This detail allowed for the close inspection of hemlocks and provided information about their chlorophyll vigor and needle mass.

The health classification with the strongest correlation was the healthy hemlock class on the non-shadowed portions of images. At this time, pixel-based image classification procedures such as supervised classifications have not proved useful in determining the percentage of damage within a stand supervised classification was performed on. More promise might lie in automated classifications of damage using image segmentation techniques.

The vegetation index that removed external parameters and normalized the data to the greatest extent is the transform normalized difference vegetation index (TNDVI). The spectral responses within the Damaged_Dark classification had the

greatest range of values of the four vegetation classes, but within the TNDVI

Damage_Dark had the tightest range of values.

It was unknown at the outset of this project whether 8-bit imagery would

preserve spectral differences between damaged and healthy hemlocks. If this was

not possible, there was speculation that 10-bit imagery might lend significant

results because of the increase in quantized levels. While 8-bit imagery preserved

spectral differences, 10-bit data did not yield any significant additional

information. The usefulness of AIMS-1 data is apparent through its preservation

of spectral differentiation between healthy and damaged hemlocks, and its spatial

resolution which allowed for these measurements to be made.

LITERATURE CITED

Abeyta, A. M., Franklin, J. (1998) The accuracy of vegetation stand boundaries derived from image segmentation in a desert environment. *Photogrammetric Engineering & Remote Sensing*, 64, pp. 59-66.

Battles, J. J., Cleavitt, N., Fahey, T. J., & Evans, R. A. (1999) Vegetation and structure in two hemlock stands threatened by the hemlock woolly adelgid. In. McManus, K.A., Shields K.S., and Souto, D. R. (Eds.), *Proceedings: Symposium on Sustainable Management of hemlock Ecosystems in Eastern North America.*, (pp. 55- 61). Newton Square, PA: USDA For. Serv.

Bonneau, L. R., Shields, K. S., & Civco, D. L. (1999a) A technique to identify changes in hemlock forest health over space and time using satellite image data. *Biological Invasions*, 1, pp. 262-279.

Bonneau, L. R., Shields, K. S., & Civco, D. L. (1999b) Using satellite images to classify and analyze the health of hemlock forests infested by the hemlock woolly adelgid. *Biological Invasions*, 1, pp. 255-267.

Division of Water Supply Protection (DWSP), Massachusetts Department of Conservation and Recreation—(2004) Hemlock Woolly Adelgid (*Adelges tsugae* Annand) on DWSP Lands: Problem Extent and Proposed Management Approach.

Elvidge, C. D., & Zhikang, C. (1995) Comparison of broad-band and narrow-band red and near-infrared vegetation indices. *Remote Sensing of the Environment*, 54, pp. 38-48.

Evans, R. A. (1995) Potential impacts of hwa on eastern hemlock ecosystems. In Salom, S. M., Tigner, T. C. & Reardon, R. C. (Eds.), *Proceedings of the First Hemlock Woolly Adelgid Review.*, (pp. 42- 57). Morgantown, WV: USDA For Serv.

Foster, D. R., & Aber, J. D. (2004) *Forests in Time*, New Haven & London: Yale University Press.

Goerlich, D. L., & Nyland, R. D. (1999) Natural regeneration of eastern hemlock: A review. In. McManus, K.A., Shields K.S., and Souto, D. R. (Eds.), *Proceedings: Symposium on Sustainable Management of hemlock Ecosystems in Eastern North America.*, (pp. 14-22). Newton Square, PA: USDA For. Serv.

Guyot, G., Guyon, D., & Riom, J. (1989) Factors affecting the spectral response of forest canopies: A review. *Geocartography International*, 3, pp. 3-18.

Haralick, R. M., Shapiro, L. G., (1985) Survey: Image segmentation techniques. *Computer Vision Graphics and Image Processing*, 29, pp. 100-132.

Horler, D. N. H., Dockray, M., & Barber, J. (1983) The red edge of plant leaf reflectance. *International Journal of Remote Sensing*, 4, pp. 273-288.

Jenkins, J. C., Aber, J. D., & Canham C. D. (1999) Hemlock woolly adelgid impacts on community structure and n cycling rates in eastern hemlock forests. *Canadian Journal of Forest Research*, 29, pp. 630- 645.

Jenkins, J. C., Canham, C. D., & Barten, P. K. (1999) Predicting long-term forest development following hemlock mortality. In. McManus, K.A., Shields K.S., and Souto, D. R. (Eds.), *Proceedings: Symposium on Sustainable Management of hemlock Ecosystems in Eastern North America.*, (pp. 62- 75). Newton Square, PA: USDA For. Serv.

Jensen, John R. (1996) *Introductory Digital Image Processing*, Upper Saddle River, NJ: Prentice Hall.

Jensen, John R. (2000) *Remote Sensing of the Environment: An Earth Resource Perspective*, Upper Saddle River, NJ: Prentice Hall.

Kizlinski, M. L., Orwig, D. A., Cobb, R. C., Foster, D. R. (2002) Direct and indirect ecosystem consequences of an invasive pest on forests dominated by eastern hemlock. *Journal of Biogeography*, 29, pp.1489-1503.

Lamar, W. R., McGraw, J. B., Warner, T. A. (2005) Multitemporal censusing of a population of eastern hemlock (*Tsuga canadensis* L.) from remotely sensed imagery using an automated segmentation and reconciliation procedure. *Remote Sensing of Environment*, 94, pp. 133-143.

Leica Geosystems GIS & Mapping, (2005) *Erdas Online Help Manual*, Atlanta, GA.

McWilliams, W. H., & Schmidt, T. L. (1999) Composition, structure, and sustainability of hemlock ecosystems in eastern north America. In. McManus, K.A., Shields K.S., and Souto, D. R. (Eds.), *Proceedings: Symposium on Sustainable Management of hemlock Ecosystems in Eastern North America.*, (pp. 5- 10). Newton Square, PA: USDA For. Serv.

Miles, P. W. (1990) Aphid salivary secretions and their involvement in plant toxicases. In. R. K. Campbell and R. D. Eikenbary (Eds.), *Aphid-plant-genotype Interactions*., (pp. 131-147). Elsevier, New York.

Millette, T. L., Hayward, C. D. (2005) Detailed forest stand metrics taken from AIMS-1 sensor data, *Proceedings: ASPRS 2005 Annual Conference*., (pp. 8).

Orwig, D. A., & Foster, D. R. (1998) Forest response to the introduced hemlock woolly adelgid in southern New England, USA. *Journal of the Torrey Botanical Society*, 125(1) pp. 60-73.

Orwig, D. A., & Foster, D. A. (1999) Stand, landscape, and ecosystem analyses of hemlock woolly adelgid outbreaks in southern New England: An overview. In McManus, K.A., Shields K.S., and Souto, D. R. (Eds.), *Proceedings: Symposium on Sustainable Management of hemlock Ecosystems in Eastern North America*., (pp. 123- 125). Newton Square, PA: USDA For. Serv.

Orwig, D. A. (2002) Ecosystem to regional impacts of introduced pests and pathogens: Historical context, questions and issues. *Journal of Biogeography*, 29, pp. 1471- 1474.

Pontius, J. (2005) Using AVIRIS to assess hemlock abundance and early decline in the Catskills, NY. In Review.

Quimby, J. W. (1995) Value and importance of hemlock ecosystems in the eastern United States. In Salom, S. M., Tigner, T. C. & Reardon, R. C. (Eds.), *Proceedings of the First Hemlock Woolly Adelgid Review*., (pp. 1-8). Morgantown, WV: USDA For Serv.

Royle, D. D. & Lathrop, R. G. (1997) Monitoring hemlock forest health in New Jersey using Landsat TM data and change detection techniques. *Forest Science*, 43, pp. 327-335.

Royle, D. D., & Lathrop, R. G.(2002a) Discriminating *Tsuga canadensis* hemlock forest defoliation using remotely sensed change detection. *Journal of Nematology*, 34, pp. 213- 221.

Royle, D. D. & Lathrop, R. G. (2002b) Using Landsat imagery to quantify temporal and spatial patterns in hemlock decline. *Proceedings: Hemlock Woolly Adelgid in the Eastern United States Symposium*. East Brunswick, NJ.

Rutgers Cooperative Extension (RCE), New Jersey Agricultural Experiment Station—(2002) The Hemlock Woolly Adelgid: Life Cycle, Monitoring, and Pest Management in New Jersey.

Schowengert, R. A. (1983) *Techniques for Image Processing and Classification in Remote Sensing*, Orlando FL: Academic Press, Inc.

Shields, K. S., Young, R. F., & Berlyn, G. P. (1995) Hemlock woolly adelgid feeding mechanisms. In Salom, S. M., Tigner, T. C. & Reardon, R. C. (Eds.), *Proceedings of the First Hemlock Woolly Adelgid Review*., (pp. 36-41). Morgantown, WV: USDA For Serv.

Souto, D., Luther, T., Chianese, B. (1995) Past and current status of hwa in eastern and Carolina hemlock stands. In Salom, S. M., Tigner, T. C. & Reardon, R. C. (Eds.), *Proceedings of the First Hemlock Woolly Adelgid Review*., (pp. 9-15). Morgantown, WV: USDA For Serv.

Winne, J. C. (1999) An automated multi-step algorithm for polygon delineation using image segmentation. University of Montana.

Woodcock, C. Harward, V. J. (1992) Nested-hierarchical scene models and image segmentation. *International Journal of Remote Sensing*, 13, pp. 3167-3187.

Yamasaki, M., DeGraaf, R. M., & Lanier, J. W. (1999) Wildlife habitat associations in eastern hemlock—Birds, smaller mammals, and forest carnivores. In. McManus, K.A., Shields K.S., and Souto, D. R. (Eds.), *Proceedings: Symposium on Sustainable Management of hemlock Ecosystems in Eastern North America*., (pp. 135- 141). Newton Square, PA: USDA For. Serv.

Yorks, T. E., Jenkins, J. C., Leopold, D. J., Raynal, D. J., & Orwig, D. A. (1999) Influences of eastern hemlock mortality on nutrient cycling. In. McManus, K.A., Shields K.S., and Souto, D. R. (Eds.), *Proceedings: Symposium on Sustainable Management of hemlock Ecosystems in Eastern North America*., (pp. 126-133). Newton Square, PA: USDA For. Serv.

Young, R. F., Shields, K. S., & Berlyn, G. P. (1995) Hemlock woolly adelgid (Homoptera: Adelgidae): Stylet bundle insertion and feeding sites. *Annals of the Entomological Society of America*, 88, pp. 827-835.

APPENDIX A

(*Table 2*): Statistics for the Mean Pixel Values in Band 1, Plot 146. Health category 1 represents healthy hemlocks and healthy category 2 represents damaged hemlocks.

Group Statistics

	HEALTH	N	Mean	Std. Deviation	Std. Error Mean
MEAN	1	75	134.31849	10.26738	1.18558
	2	76	78.05443	10.59999	1.21590

Independent Samples Test

		Levene's Test for Equality of Variances		t-test for Equality of Means						
									95% Confidence Interval of the Difference	
		F	Sig.	t	df	Sig. (2-tailed)	Mean Difference	Std. Error Difference	Lower	Upper
MEAN	Equal variances assumed	.192	.662	33.124	149	.000	56.26406	1.69860	52.90761	59.62051
	Equal variances not assumed			33.131	148.949	.000	56.26406	1.69824	52.90831	59.61981

(*Table 3*): Statistics for the Maximum Pixel Values in Band 1, Plot 146. Health category 1 represents healthy hemlocks and healthy category 2 represents damaged hemlocks.

Group Statistics

	HEALTH	N	Mean	Std. Deviation	Std. Error Mean
MAXIMUM	1	75	169.55	10.96	1.27
	2	76	125.45	12.98	1.49

Independent Samples Test

		Levene's Test for Equality of Variances		t-test for Equality of Means						95% Confidence Interval of the Difference	
		F	Sig.	t	df	Sig. (2-tailed)	Mean Difference	Std. Error Difference	Lower	Upper
MAXIMUM	Equal variances assumed	3.241	.074	22.546	149	.000	44.10	1.96	40.23	47.96
	Equal variances not assumed			22.572	145.533	.000	44.10	1.95	40.24	47.96

(*Table 4*): Statistics for the Mean Values in Band 2, Plot 146. Health category 1 represents healthy hemlocks and healthy category 2 represents damaged hemlocks.

Group Statistics

	HEALTH	N	Mean	Std. Deviation	Std. Error Mean
MEAN	1	75	40.54	3.91	.45
	2	76	44.03	6.77	.78

Independent Samples Test

		Levene's Test for Equality of Variances		t-test for Equality of Means						
									95% Confidence Interval of the Difference	
		F	Sig.	t	df	Sig. (2-tailed)	Mean Difference	Std. Error Difference	Lower	Upper
MEAN	Equal variances assumed	17.802	.000	-3.871	149	.000	-3.49	.90	-5.27	-1.71
	Equal variances not assumed			-3.884	120.285	.000	-3.49	.90	-5.27	-1.71

(*Table 5*): Statistics for the Maximum Pixel Values in Band 2, Plot 146. Health category 1 represents healthy hemlocks and healthy category 2 represents damaged hemlocks.

Group Statistics

	HEALTH	N	Mean	Std. Deviation	Std. Error Mean
MAXIMUM	1	75	58.39	5.73	.66
	2	76	72.12	9.41	1.08

Independent Samples Test

		Levene's Test for Equality of Variances		t-test for Equality of Means							
										95% Confidence Interval of the Difference	
		F	Sig.	t	df	Sig. (2-tailed)	Mean Difference	Std. Error Difference	Lower	Upper
MAXIMUM	Equal variances assumed	12.476	.001	-10.816	149	.000	-13.73	1.27	-16.24	-11.22
	Equal variances not assumed			-10.849	124.211	.000	-13.73	1.27	-16.24	-11.23

(*Table 6*): Statistics for the Mean Pixel Values in Band 1, Plot 165. Health category 1 represents healthy hemlocks and healthy category 2 represents damaged hemlocks.

Group Statistics

	HEALTH	N	Mean	Std. Deviation	Std. Error Mean
MEAN	1	62	142.81392	11.14007	1.41479
	2	60	99.47437	13.59421	1.75500

Independent Samples Test

		Levene's Test for Equality of Variances		t-test for Equality of Means						
									95% Confidence Interval of the Difference	
		F	Sig.	t	df	Sig. (2-tailed)	Mean Difference	Std. Error Difference	Lower	Upper
MEAN	Equal variances assumed	4.336	.039	19.288	120	.000	43.33955	2.24695	38.89076	47.78835
	Equal variances not assumed			19.226	114.025	.000	43.33955	2.25426	38.87390	47.80521

(*Table 7*): Statistics for the Maximum Pixel Values in Band 1, Plot 165. Health category 1 represents healthy hemlocks and healthy category 2 represents damaged hemlocks.

Group Statistics

	HEALTH	N	Mean	Std. Deviation	Std. Error Mean
MAXIMUM	1	62	187.32	15.17	1.93
	2	60	144.92	16.72	2.16

Independent Samples Test

		Levene's Test for Equality of Variances		t-test for Equality of Means						
									95% Confidence Interval of the Difference	
		F	Sig.	t	df	Sig. (2-tailed)	Mean Difference	Std. Error Difference	Lower	Upper
MAXIMUM	Equal variances assumed	.535	.466	14.680	120	.000	42.41	2.89	36.69	48.13
	Equal variances not assumed			14.657	118.012	.000	42.41	2.89	36.68	48.14

(*Table 8*): Statistics for the Mean Values in Band 2, Plot 165. Health category 1 represents healthy hemlocks and healthy category 2 represents damaged hemlocks.

Group Statistics

	HEALTH	N	Mean	Std. Deviation	Std. Error Mean
MEAN	1	62	47.84419	5.01708	.63717
	2	60	60.44455	11.19311	1.44502

Independent Samples Test

		Levene's Test for Equality of Variances		t-test for Equality of Means							
										95% Confidence Interval of the Difference	
		F	Sig.	t	df	Sig. (2-tailed)	Mean Difference	Std. Error Difference	Lower	Upper
MEAN	Equal variances assumed	42.142	.000	-8.067	120	.000	-12.60036	1.56199	-15.69298	-9.50773
	Equal variances not assumed			-7.979	81.204	.000	-12.60036	1.57927	-15.74248	-9.45823

(*Table 9*): T-Test performed on the means of all trees labeled as damaged (Healthy Class 2) and all trees labeled healthy (Healthy Class 1).

Group Statistics

	HEALTH	N	Mean	Std. Deviation	Std. Error Mean
MEAN	1	257	135.13432	20.31220	1.26704
	2	190	102.37667	19.38262	1.40616

Independent Samples Test

		Levene's Test for Equality of Variances		t-test for Equality of Means						95% Confidence Interval of the Difference	
		F	Sig.	t	df	Sig. (2-tailed)	Mean Difference	Std. Error Difference		Lower	Upper
MEAN	Equal variances assumed	.045	.832	17.185	445	.000	32.75765	1.90616		29.01146	36.50383
	Equal variances not assumed			17.306	417.369	.000	32.75765	1.89280		29.03704	36.47825

(*Figure 27*): Output images of the three vegetation indices used to test which index would provide the most information about hemlock damage. Images in this figure represent Plot 146.


a. NDVI Normalized Difference Index

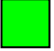b. SAVI (Soil Adjusted Vegetation Index)
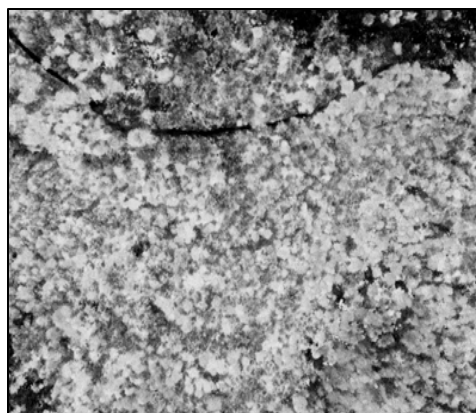
c. TNDVI (Transform NDVI

(*Figure 28*): Output images of the three vegetation indices used to test which index would provide the most information about hemlock damage. Images in this figure represent Plot 165.
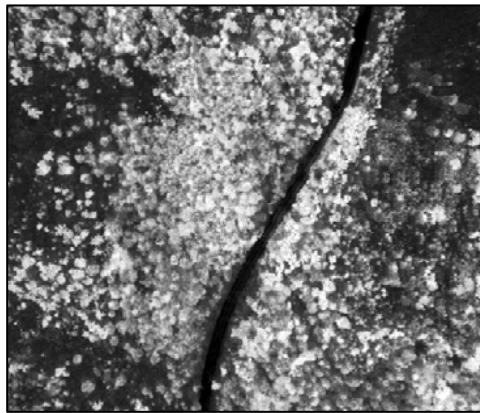
a. NDVI Normalized Difference Index   b. SAVI (Soil Adjusted Vegetation Index)
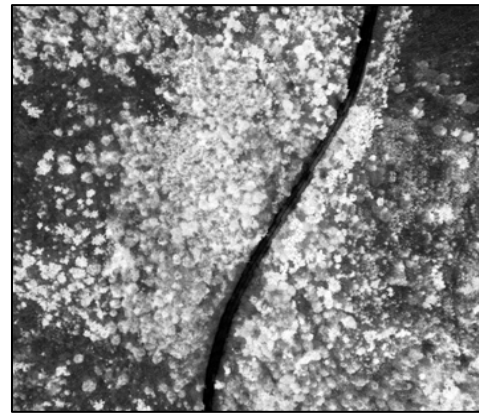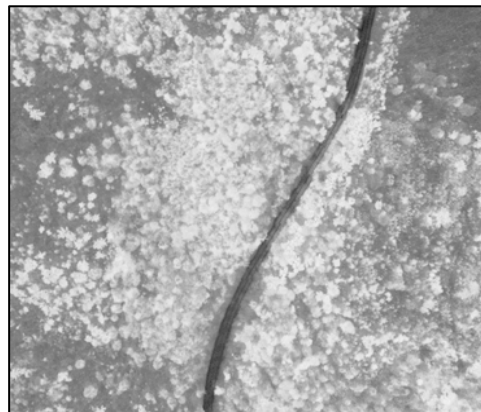
c. TNDVI (Transform NDVI)

(*Figure 29*): Output images of the three vegetation indices used to test which index would provide the most information about hemlock damage. Images in this figure represent Plot 169.
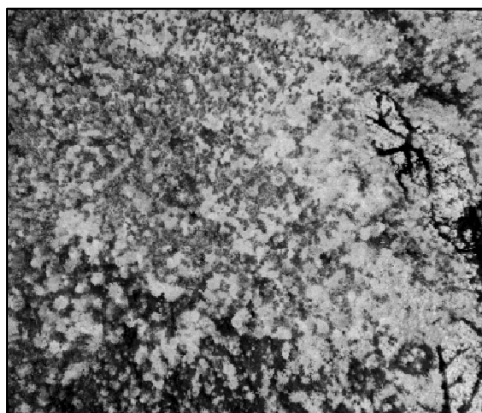
a. NDVI Normalized Difference Index   b. SAVI (Soil Adjusted Vegetation Index)
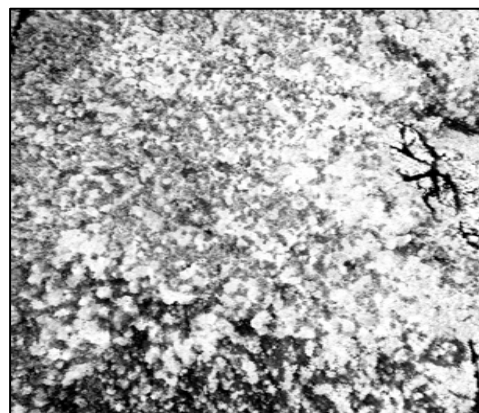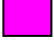
c. TNDVI (Transform NDVI)

(*Figure 30*): Supervised Classification of the subset of Plot 165. A corresponding table of what each represented color translates to on the ground can be found within Table 10, located on the next page. Supervised Classifications are described within the Methods section and the Introduction.
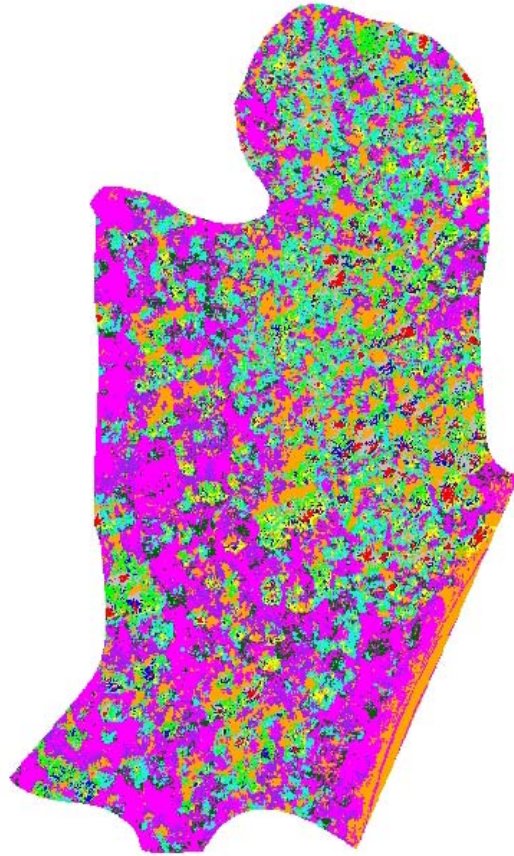
(*Table 10*): Table providing classification information for each color represented in the Supervised Classification image on the previous page.

Classification	Color In the Image		Corresponding True Life Classification
Healthy_1	Gray		Shadows on healthy hemlocks.
Healthy_2	Red		Very bright/ healthy vegetation
Healthy_3	Green		Brightest reflectance values- Appear for all White Pines
Healthy_4	Blue		Also on healthy hemlocks/ no noticeable difference between red class
Healthy_5	Yellow		Found on fringes of healthy hemlocks/ no difference from red or blue classification
Unhealthy_1	Purple		Shadows around vegetated ground
Unhealthy_2	Orange		Pavement and dark shadow areas
Unhealthy_3	Cyan		Vegetated ground cover/ including both shrubs and damaged hemlocks
Unhealthy_4	Magenta		Bare ground cover/ dirt
Unhealthy_5	Dark Green		Picks up some lighter pixels and damage/ for the most part not useful.